Sicilian Apennines


APAT
Agenzia per la Protezione dell'Ambiente e per i Servizi Tecnici
Dipartimento Difesa del Suolo
Servizio Geologico d'Italia
GEOLOGICAL MAP OF ITALY
1:1 250 000 Scale
MAIN TECTONO-STRATIGRAPHIC UNITS
SPECIALLY PRINTED FOR THE 32nd INTERNATIONAL GEOLOGICAL CONGRESS
ITALIA 2004

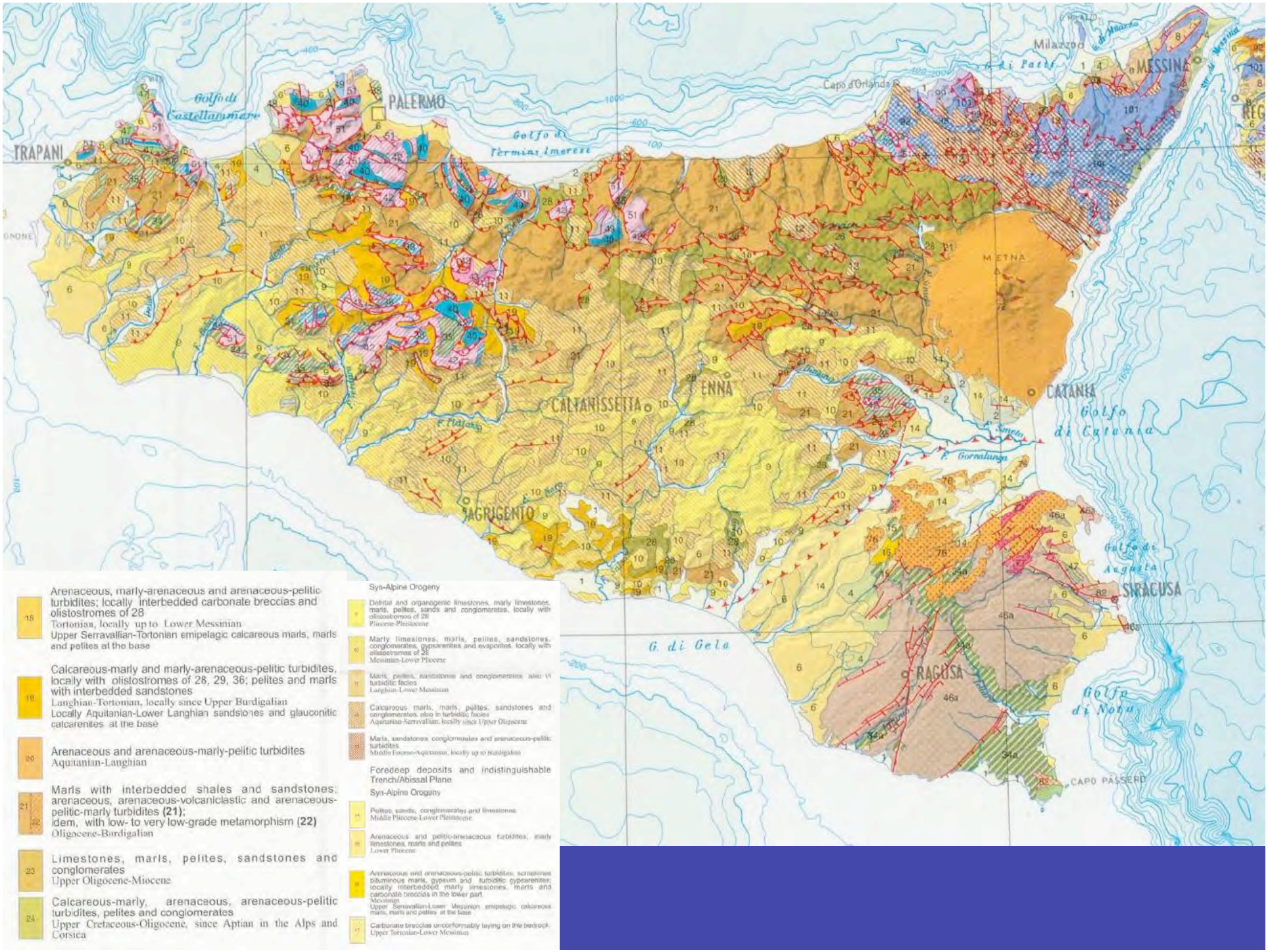

18 Arenaceous, marly-arenaceous and arenaceous-pelitic turbidites; locally interbedded carbonate breccias and olistostromes of 28
Tortonian, locally up to Lower Messinian
Upper Serravallian-Tortonian emipelagic calcareous marls, marls and pelites at the base

19 Calcareous-marly and marly-arenaceous-pelitic turbidites, locally with olistostromes of 28, 29, 36; pelites and marls with interbedded sandstones
Langhian-Tortonian, locally since Upper Burdigalian
Locally Aquitanian-Lower Langhian sandstones and glauconitic calcarenites at the base

20 Arenaceous and arenaceous-marly-pelitic turbidites
Aquitanian-Langhian

21 22 Marls with interbedded shales and sandstones; arenaceous, arenaceous-volcaniclastic and arenaceous-pelitic-marly turbidites **(21)**;
idem, with low- to very low-grade metamorphism **(22)**
Oligocene-Burdigalian

23 Limestones, marls, pelites, sandstones and conglomerates
Upper Oligocene-Miocene

24 Calcareous-marly, arenaceous, arenaceous-pelitic turbidites, pelites and conglomerates
Upper Cretaceous-Oligocene, since Aptian in the Alps and Corsica

Syn-Alpine Orogeny

9 Detrital and organogenic limestones, marly limestones, marls, pelites, sands and conglomerates, locally with olistostromes of 28
Pliocene-Pleistocene

10 Marly limestones, marls, pelites, sandstones, conglomerates, gypsarenites and evaporites, locally with olistostromes of 28
Messinian-Lower Pliocene

11 Marls, pelites, sandstones and conglomerates, also in turbiditic facies
Langhian-Lower Messinian

12 Calcareous marls, marls, pelites, sandstones and conglomerates, also in turbiditic facies
Aquitanian-Serravallian, locally since Upper Oligocene

13 Marls, sandstones, conglomerates and arenaceous-pelitic turbidites
Middle Eocene-Aquitanian, locally up to Burdigalian

Foredeep deposits and indistinguishable Trench/Abissal Plane

Syn-Alpine Orogeny

14 Pelites, sands, conglomerates and limestones
Middle Pliocene-Lower Pleistocene

15 Arenaceous and pelitic-arenaceous turbidites, marly limestones, marls and pelites
Lower Pliocene

16 Arenaceous and arenaceous-pelitic turbidites, sometimes bituminous marls, gypsum and turbiditic gypsarenites; locally interbedded marly limestones, marls and carbonate breccias in the lower part
Messinian
Upper Serravallian-Lower Messinian emipelagic calcareous marls, marls and pelites at the base

17 Carbonate breccias unconformably laying on the bedrock
Upper Tortonian-Lower Messinian

Sicily Channel

http://eol.jsc.nasa.gov/

Sicily and Calabria

http://eol.jsc.nasa.gov/

http://eol.jsc.nasa.gov/

Mondello, Sicily

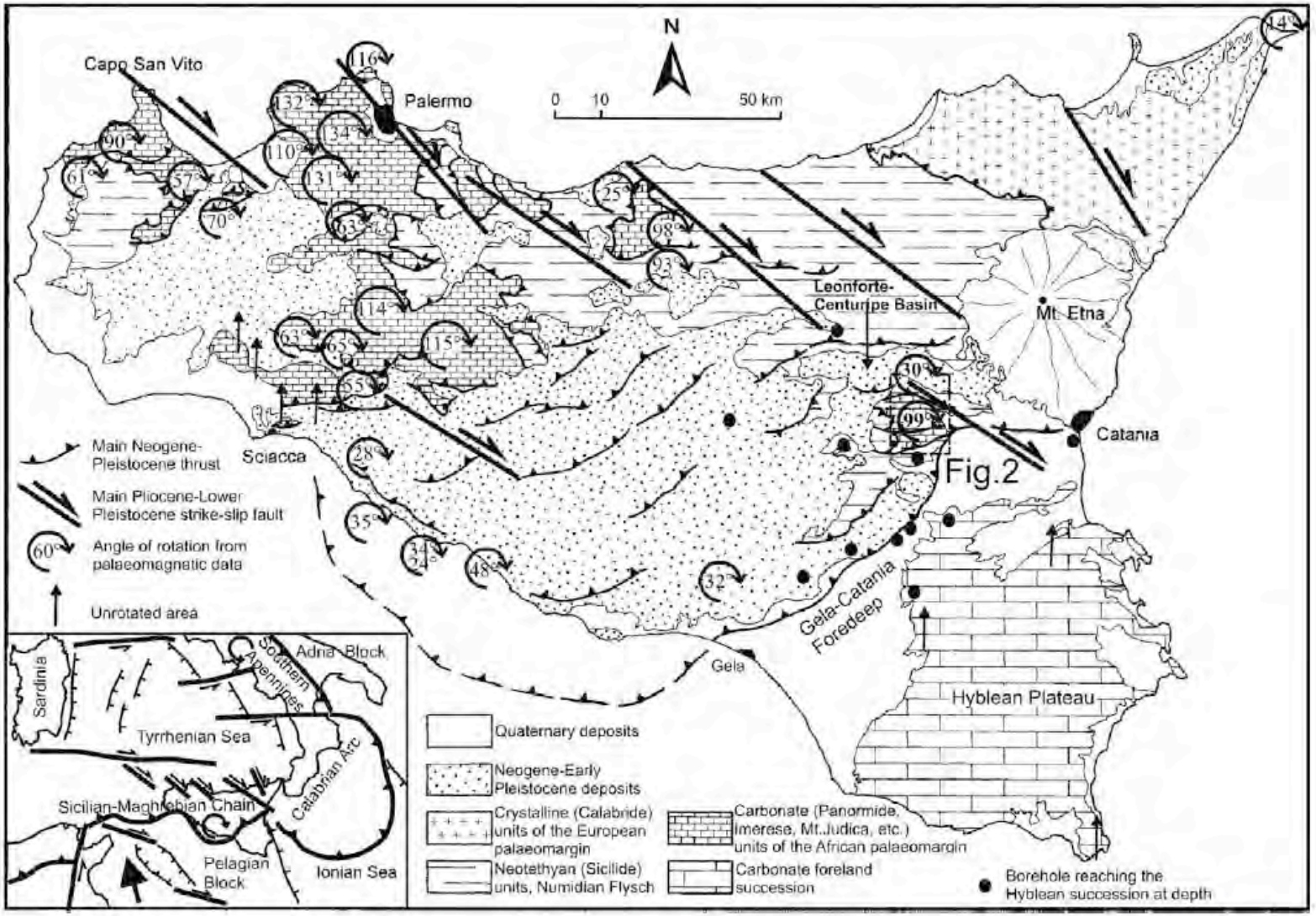

Fig. 1. Schematic geological map of Sicily. Circular arrows (and the enclosed angle) indicate the amount of clockwise rotations calculated by palaeomagnetic analyses (from Speranza et al., 1999, 2003 and references therein). Vertical arrows indicate unrotated areas. Borehole location from Bello et al. (2000). The inset shows a simplified model of lateral extrusion of the Calabrian Arc produced by the indentation of the Pelagian Block and by consequent opening of the Tyrrhenian Basin (from Catalano et al., 2004, modified). The large arrow shows the Late Tortonian to Present direction of convergence between Africa and Europe (from Mazzoli and Helman, 1994); circular arrows indicate the clockwise and counterclockwise orogen-scale rotations of the Sicilian–Maghrebides and Southern Apennines, respectively. Lines with triangles represent the front of the chain; lines with arrows the main Plio-Pleistocene strike-slip faults; lines with barbs the main Quaternary faults.

Monaco and De Guidi 2006

Monaco and De Guidi 2006

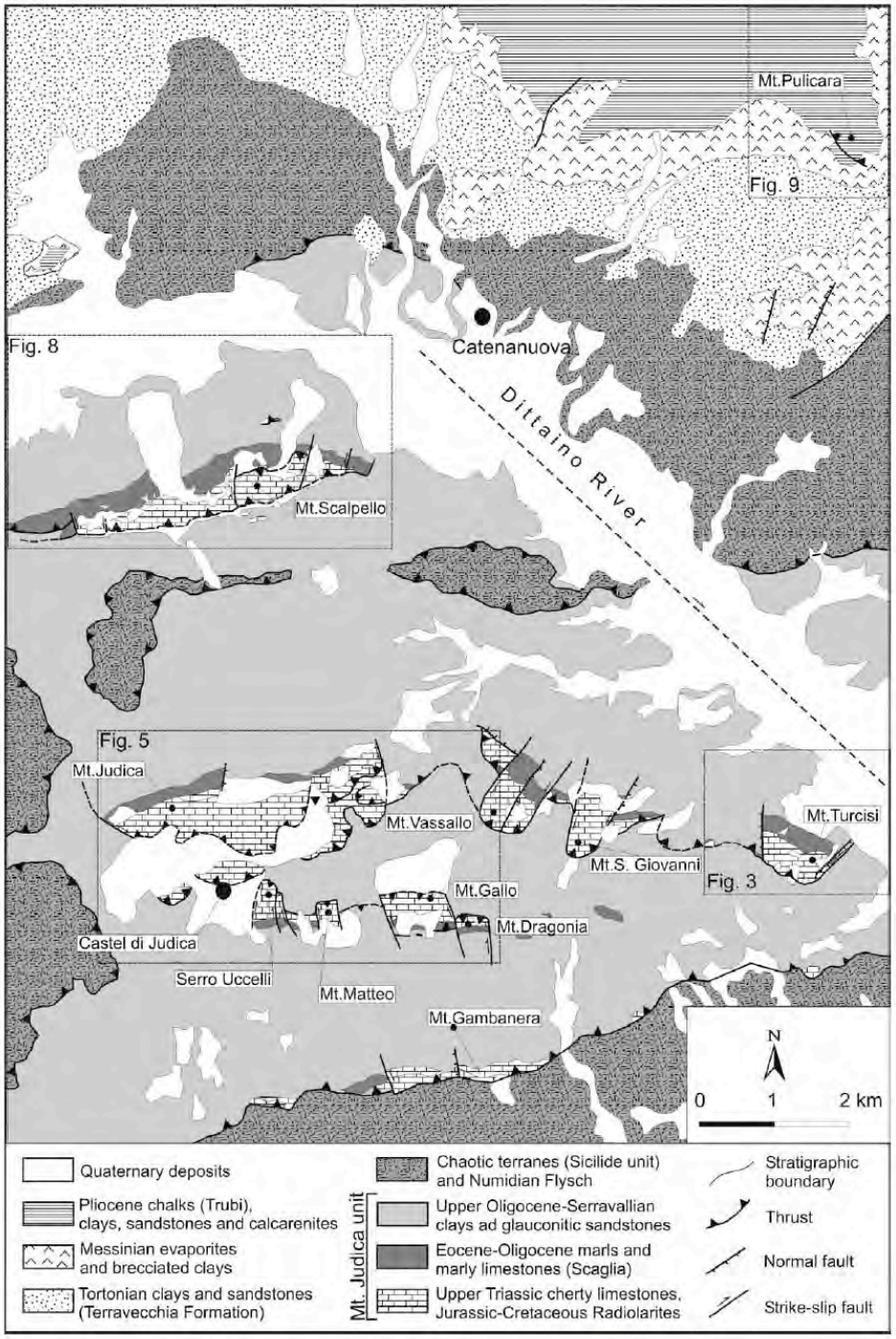

Fig. 2. Geological map of the Mt. Judica–Mt. Pulicara area (see Fig. 1 for location).

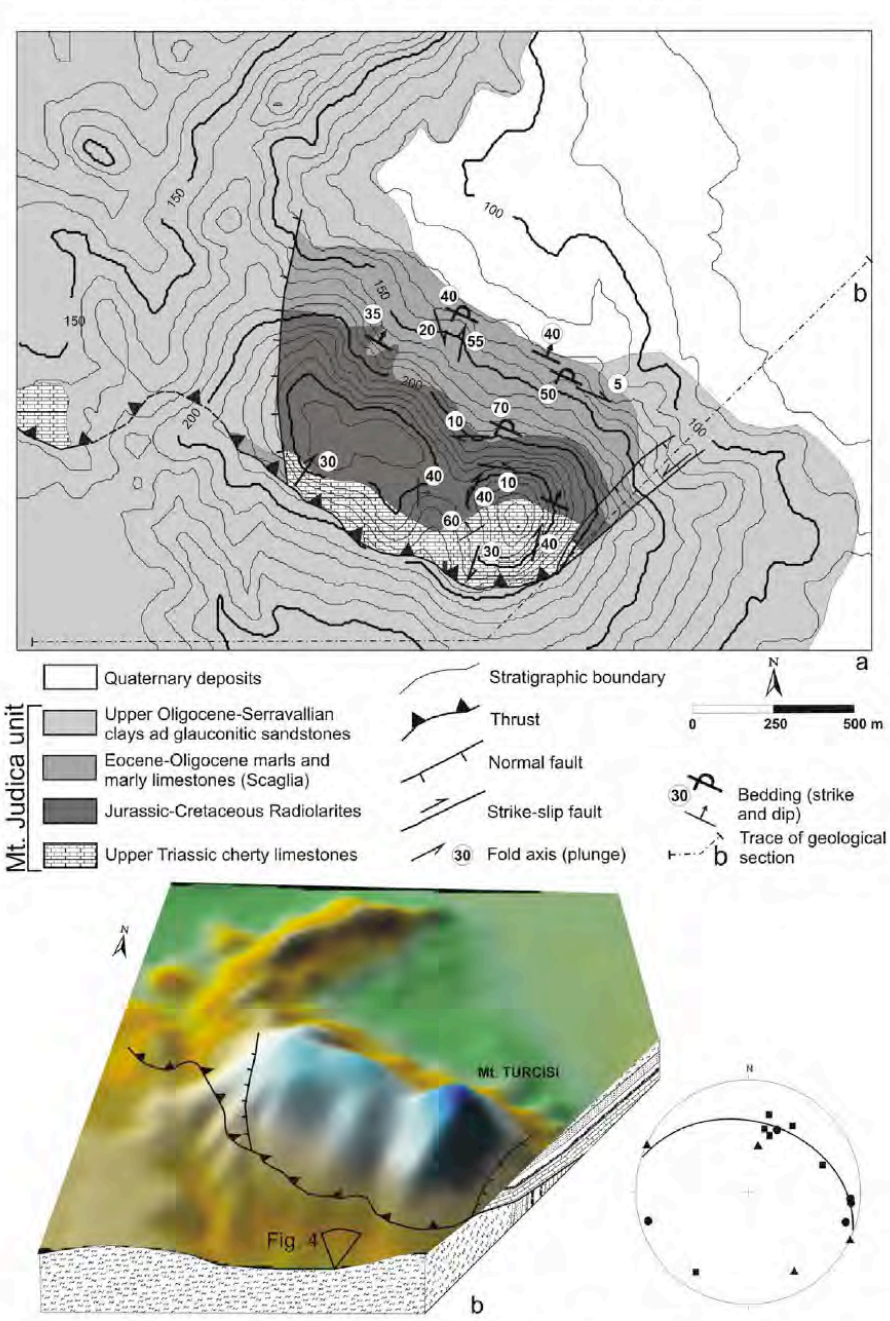

Fig. 3. (a) Geological–structural sketch map of Mt. Turcisi (see Fig. 2 for location); (b) view from the south of Mt. Turcisi ridge by the 3D prospective projection mode of a Digital Elevation Model (DEM). The stereoplot (Schmidt, lower emisphere) shows projections of the basal thrust and of beta fold axes on Calcari con selce (squares), radiolarites (triangles) and Scaglia (circles).

Monaco and De Guidi 2006

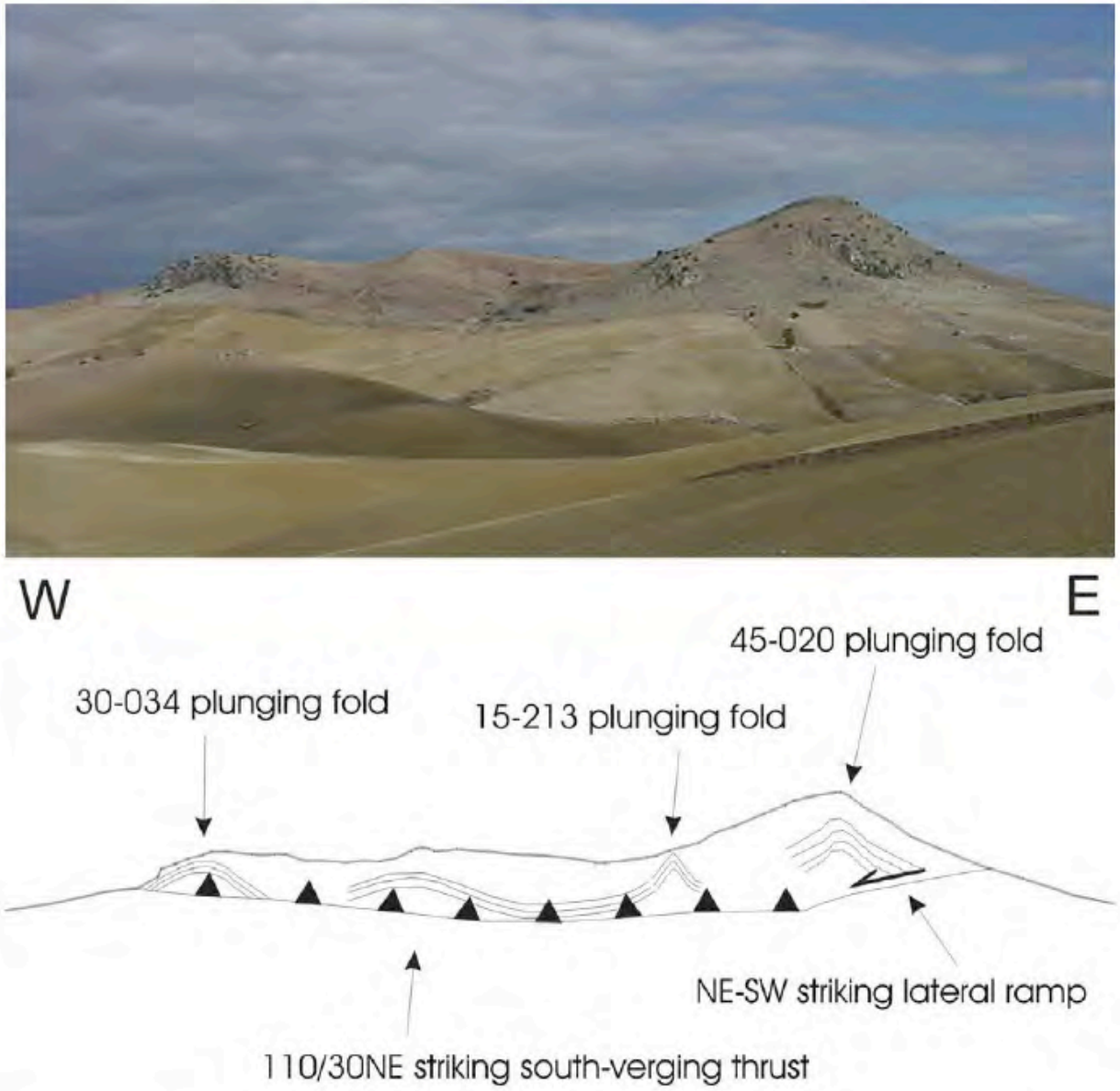

4. Panoramic view of the southern slope of Mt. Turcisi (see Fig. 3 for location). The folds of the first phase, truncated by the basal thrust, are evidenced.

Monaco and De Guidi 2006

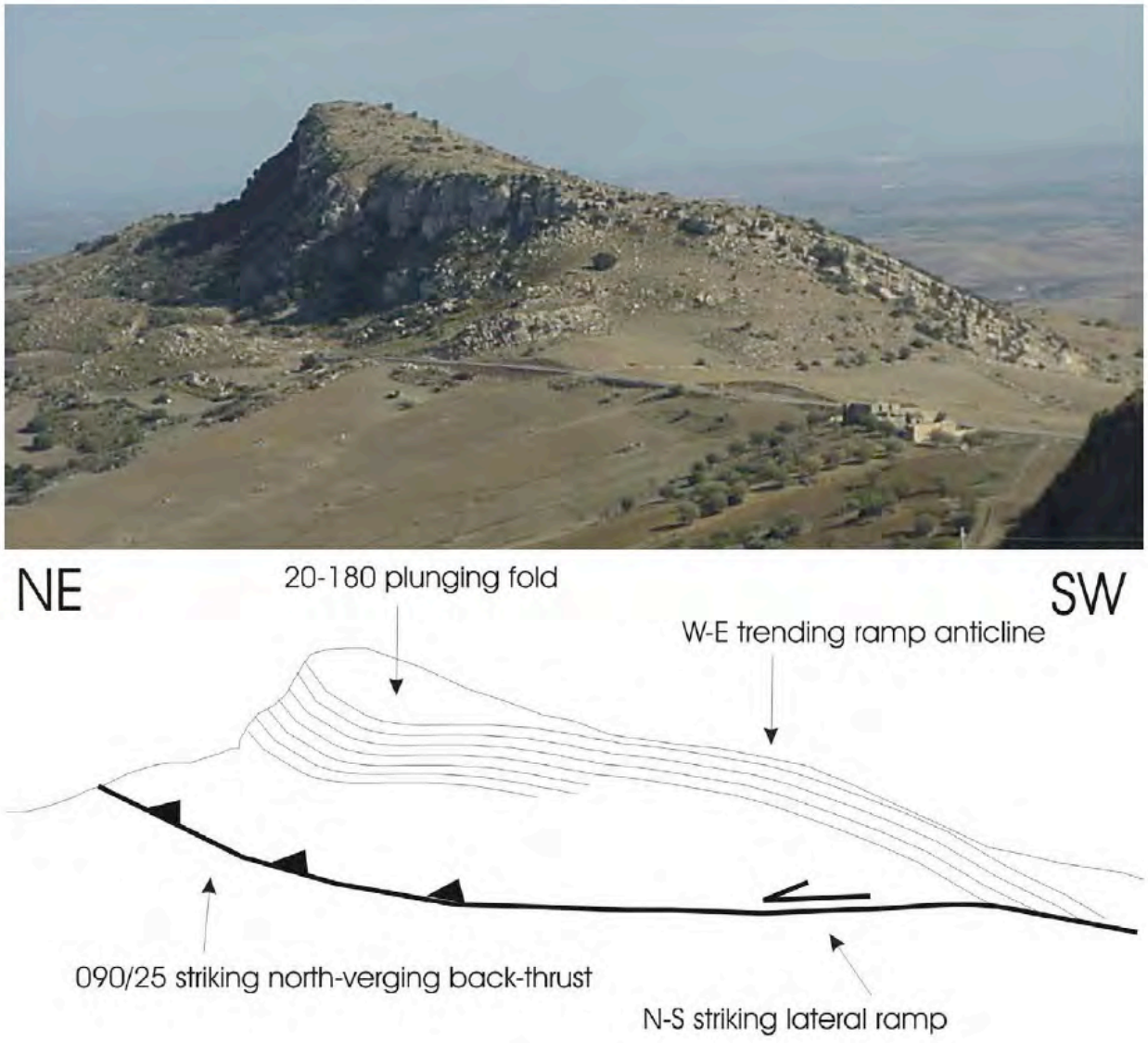

Fig. 6. Panoramic view of the northern slope of Mt. Gallo (see Fig. 5 for location). The fold of the first phase, refolded by the ramp anticline of the basal back-thrust, is evidenced.

Monaco and De Guidi 2006

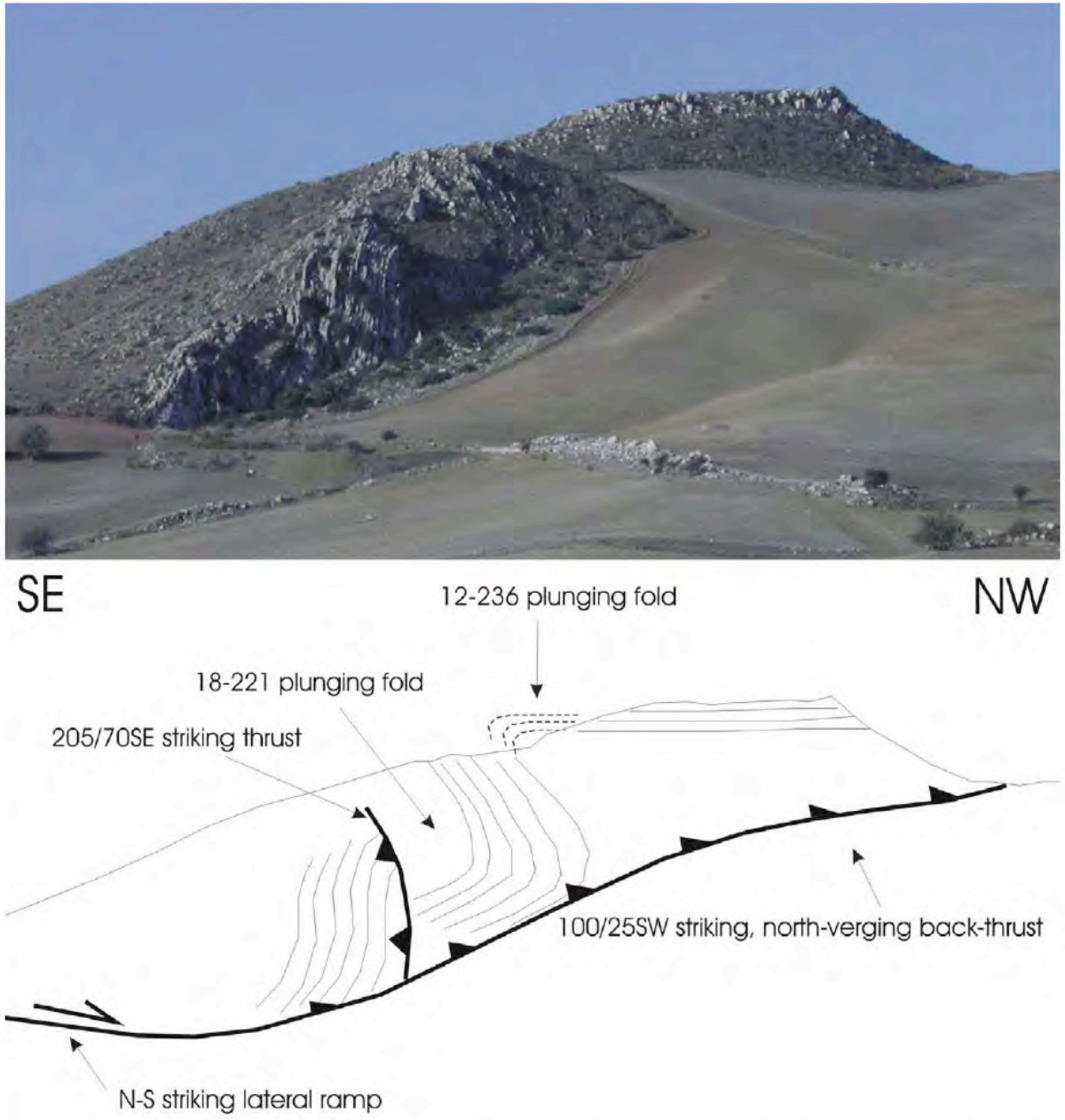

Fig. 7. Panoramic view of the northern slope of Mt. Dragonia (see Fig. 5 for location). The folds and thrust of the first phase, truncated by the basal back-thrust, are evidenced.

Monaco and De Guidi 2006

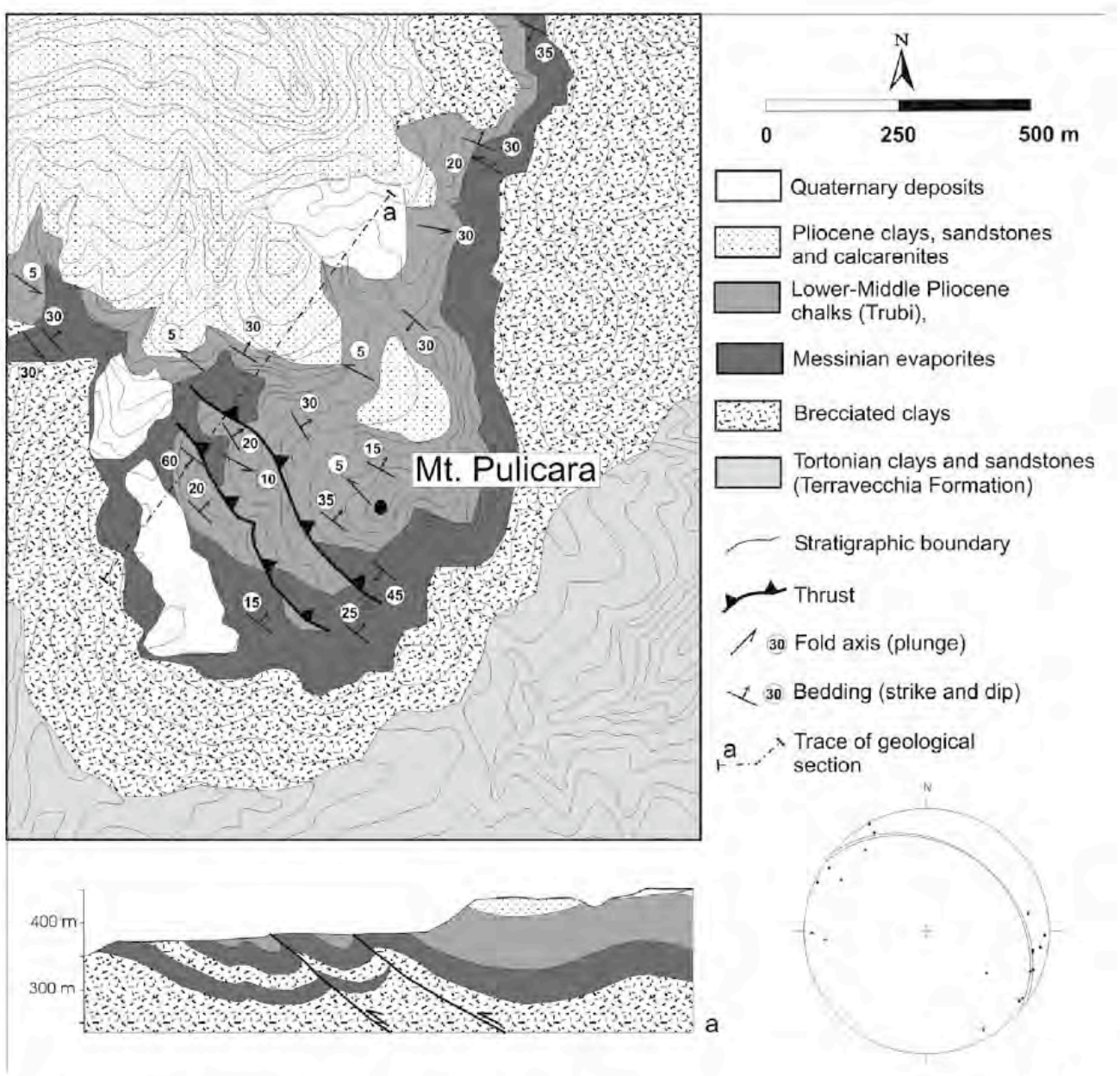

Fig. 9. Geological–structural sketch map of Mt. Pulicara (see Fig. 2 for location). The stereoplot (Schmidt, lower emisphere) shows projections of beta fold axes and of thrust planes.

Monaco and De Guidi 2006

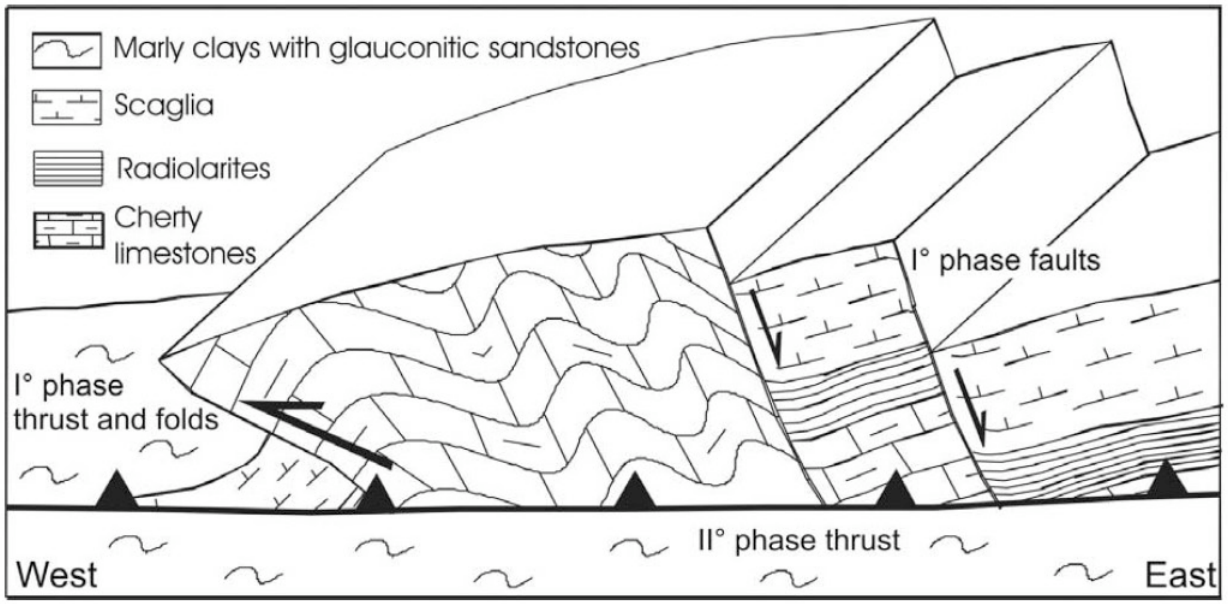

Fig. 10. Simplified kinematic model of relationships between first phase structures and basal thrust (second phase) along the Mt. Judica–Mt. Turcisi ridge; the latter propagates along different stratigraphic level.

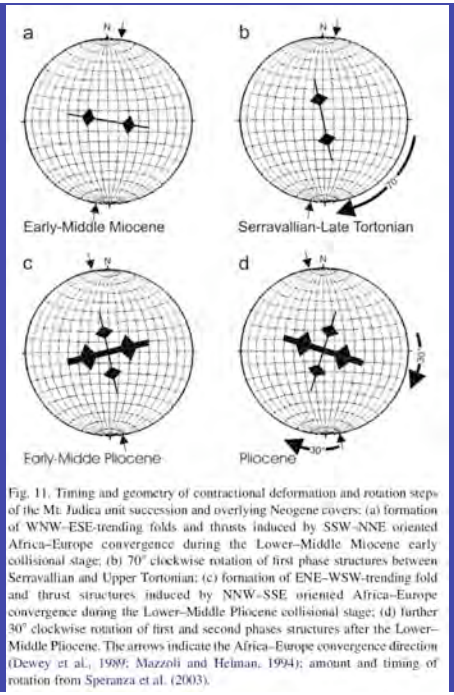

Fig. 11. Timing and geometry of contractional deformation and rotation steps of the Mt. Judica unit succession and overlying Neogene covers: (a) formation of WNW–ESE-trending folds and thrusts induced by SSW–NNE oriented Africa–Europe convergence during the Lower–Middle Miocene early collisional stage; (b) 70° clockwise rotation of first phase structures between Serravallian and Upper Tortonian; (c) formation of ENE–WSW-trending fold and thrust structures induced by NNW–SSE oriented Africa–Europe convergence during the Lower–Middle Pliocene collisional stage; (d) further 30° clockwise rotation of first and second phases structures after the Lower–Middle Pliocene. The arrows indicate the Africa–Europe convergence direction (Dewey et al., 1989; Mazzoli and Helman, 1994); amount and timing of rotation from Speranza et al. (2003).

Monaco and De Guidi 2006

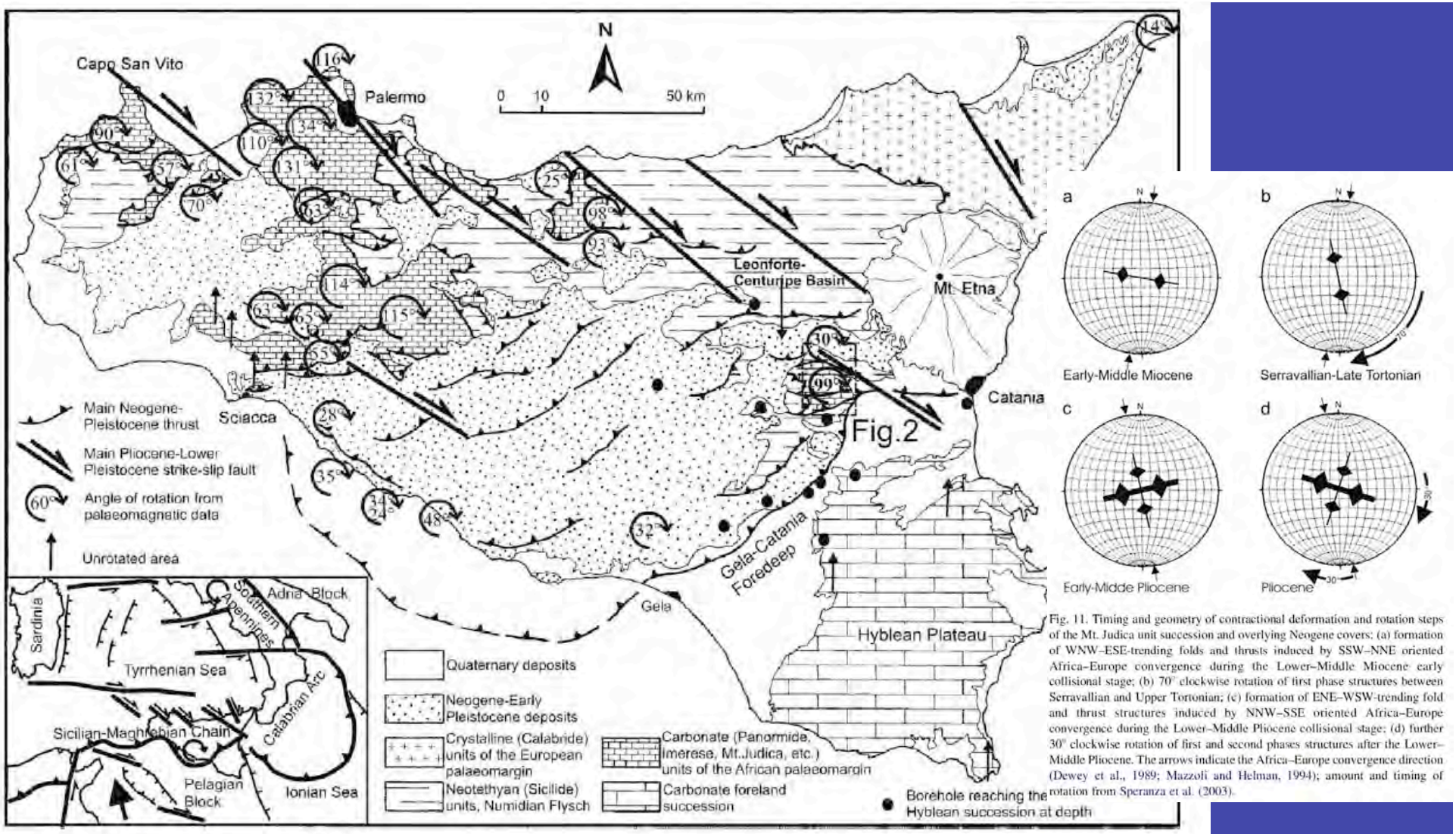

Fig. 11. Timing and geometry of contractional deformation and rotation steps of the Mt. Judica unit succession and overlying Neogene covers: (a) formation of WNW–ESE-trending folds and thrusts induced by SSW–NNE oriented Africa–Europe convergence during the Lower–Middle Miocene early collisional stage; (b) 70° clockwise rotation of first phase structures between Serravallian and Upper Tortonian; (c) formation of ENE–WSW-trending fold and thrust structures induced by NNW–SSE oriented Africa–Europe convergence during the Lower–Middle Pliocene collisional stage; (d) further 30° clockwise rotation of first and second phases structures after the Lower–Middle Pliocene. The arrows indicate the Africa–Europe convergence direction (Dewey et al., 1989; Mazzoli and Helman, 1994); amount and timing of rotation from Speranza et al. (2003).

g. 1. Schematic geological map of Sicily. Circular arrows (and the enclosed angle) indicate the amount of clockwise rotations calculated by palaeomagnetic alyses (from Speranza et al., 1999, 2003 and references therein). Vertical arrows indicate unrotated areas. Borehole location from Bello et al. (2000). The inset ows a simplified model of lateral extrusion of the Calabrian Arc produced by the indentation of the Pelagian Block and by consequent opening of the Tyrrhenian asin (from Catalano et al., 2004, modified). The large arrow shows the Late Tortonian to Present direction of convergence between Africa and Europe (from azzoli and Helman, 1994); circular arrows indicate the clockwise and counterclockwise orogen-scale rotations of the Sicilian–Maghrebides and Southern ennines, respectively. Lines with triangles represent the front of the chain; lines with arrows the main Plio-Pleistocene strike-slip faults; lines with barbs the main uaternary faults.

Monaco and De Guidi 2006

Paleogeographic evolution of the Western Mediterranean region since late Eocene (after Gelabert et al., 2002; Vera, 2004, redrawn and modified), reconstructed on the basis of paleomagnetic, structural, and bathymetric data (Oldow et al., 1990; Platzman et a...

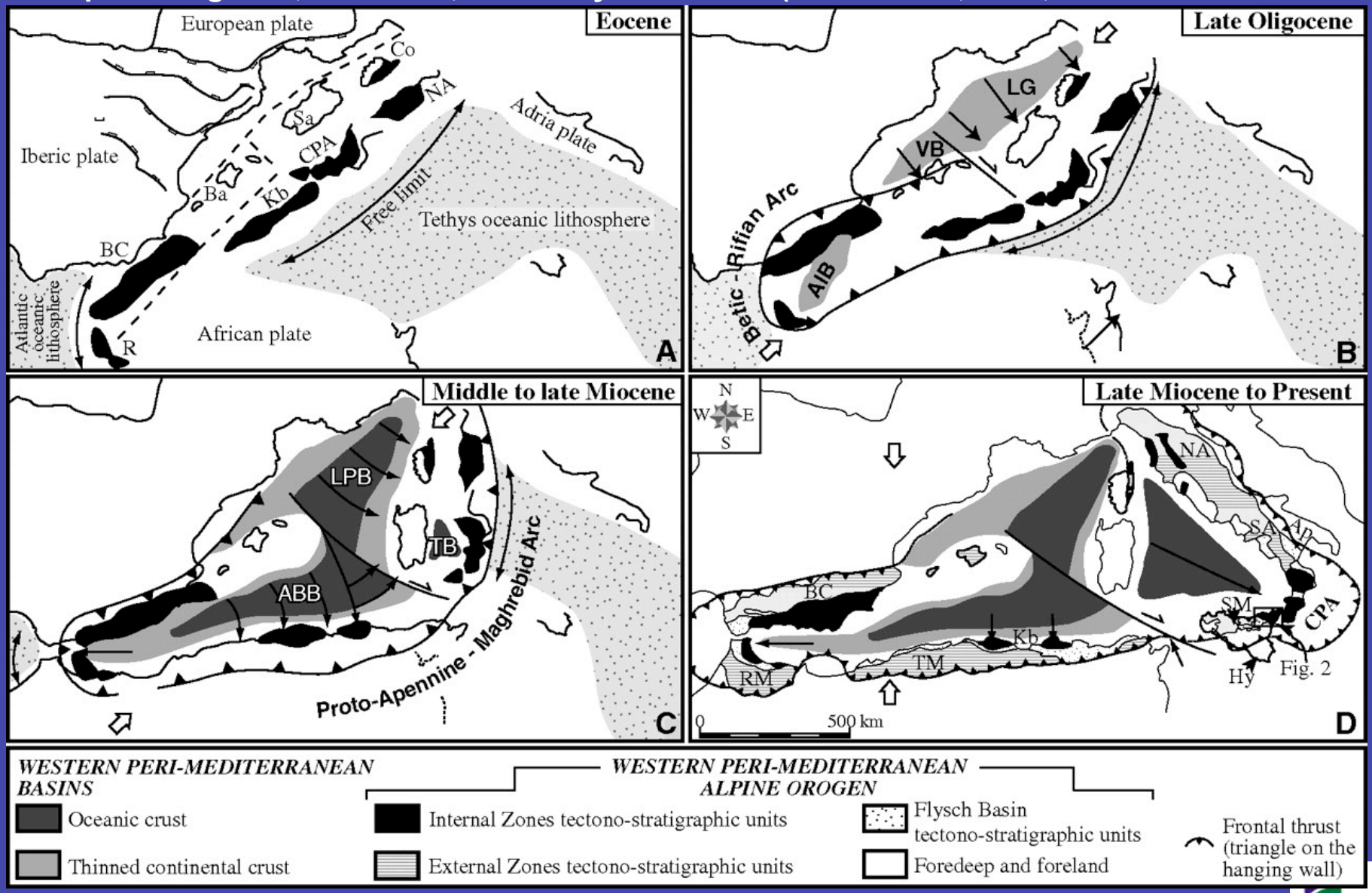

Aldega L et al. Geological Society of America Bulletin 2010;123:132-149

Geological sketch map of the Peloritani Mountains with sampling sites and traces of cross sections, redrawn and modified after Lentini et al.

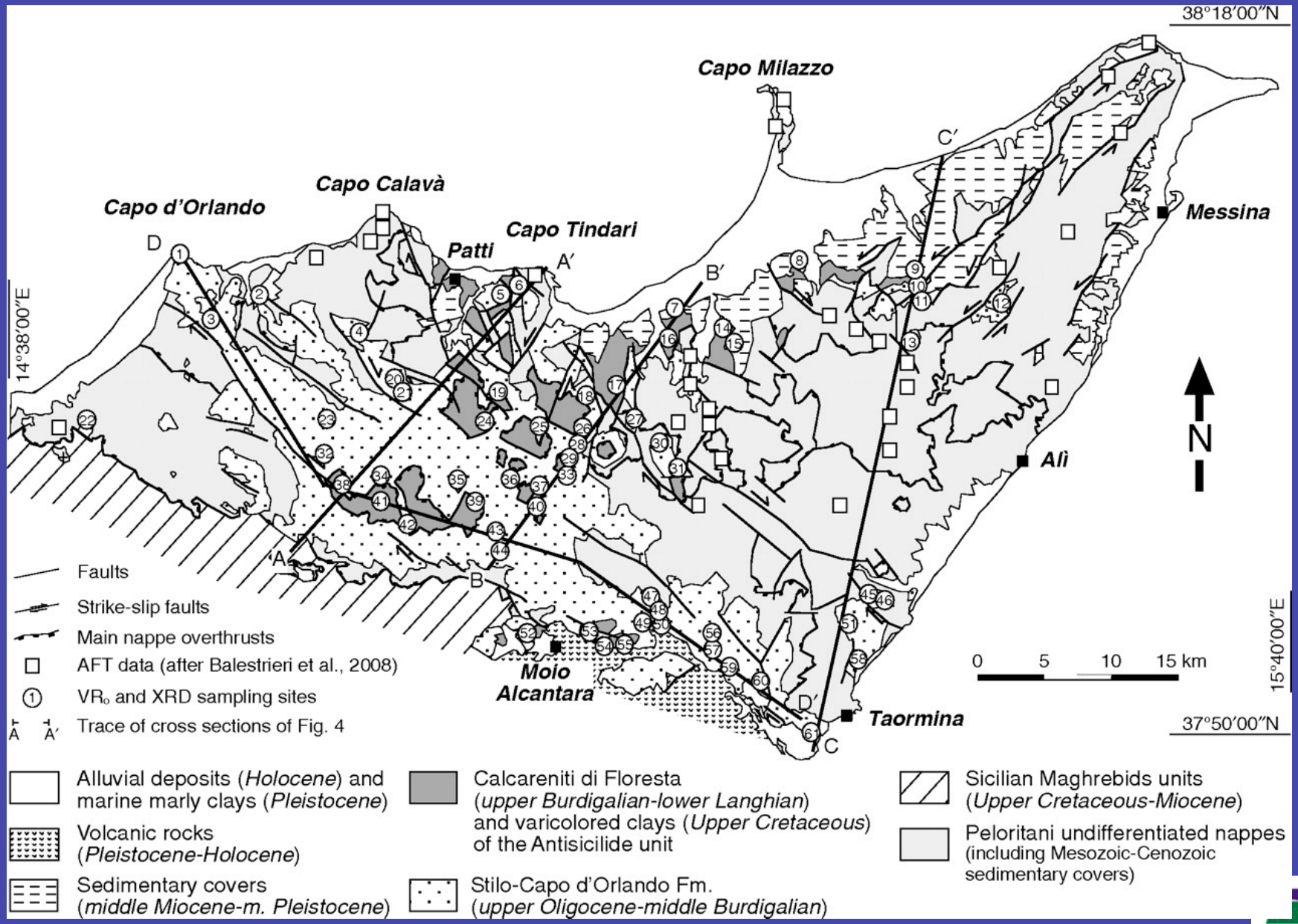

Aldega L et al. Geological Society of America Bulletin 2010;123:132-149

Schematic stratigraphic setting of the Peloritani Mountain units.

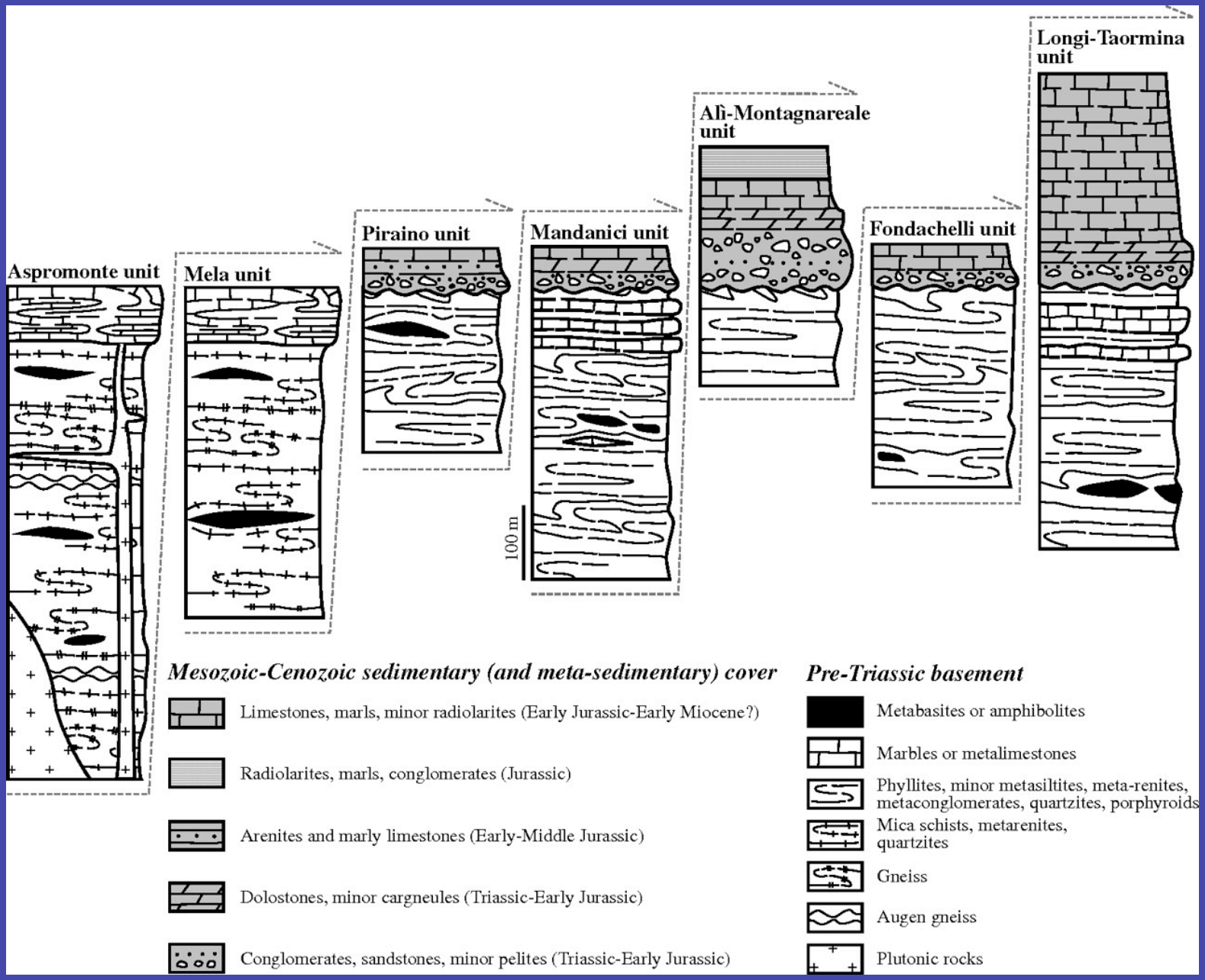

Aldega L et al. Geological Society of America Bulletin 2010;123:132-149

Geological cross sections.

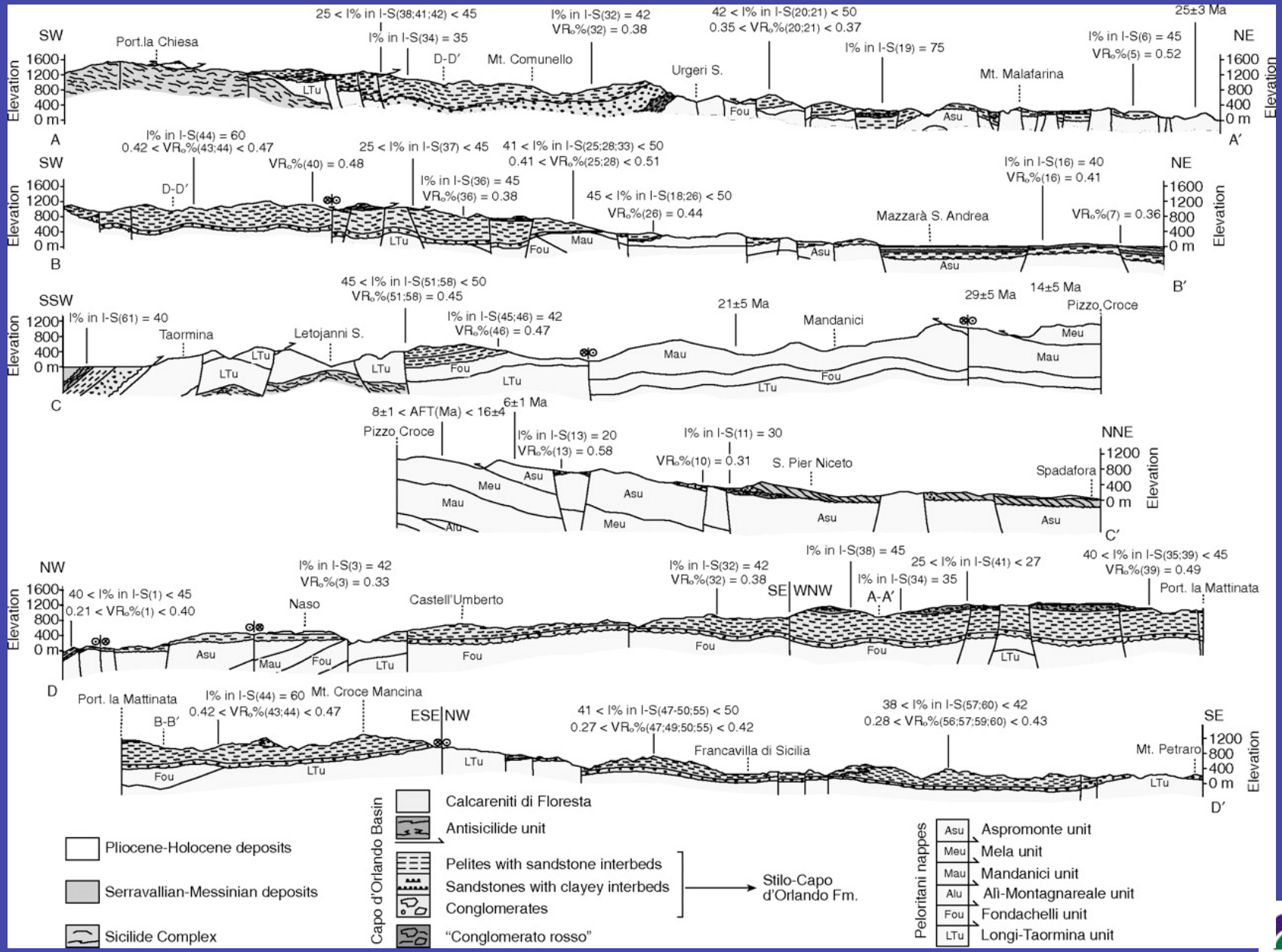

Aldega L et al. Geological Society of America Bulletin 2010;123:132-149

Synthetic stratigraphic log of the Stilo-Capo d'Orlando Formation with selected vitrinite reflectance histograms (A, C, E) and X-ray diffraction (XRD) oriented patterns of the <2 µm grain-size fraction (B, D, F).

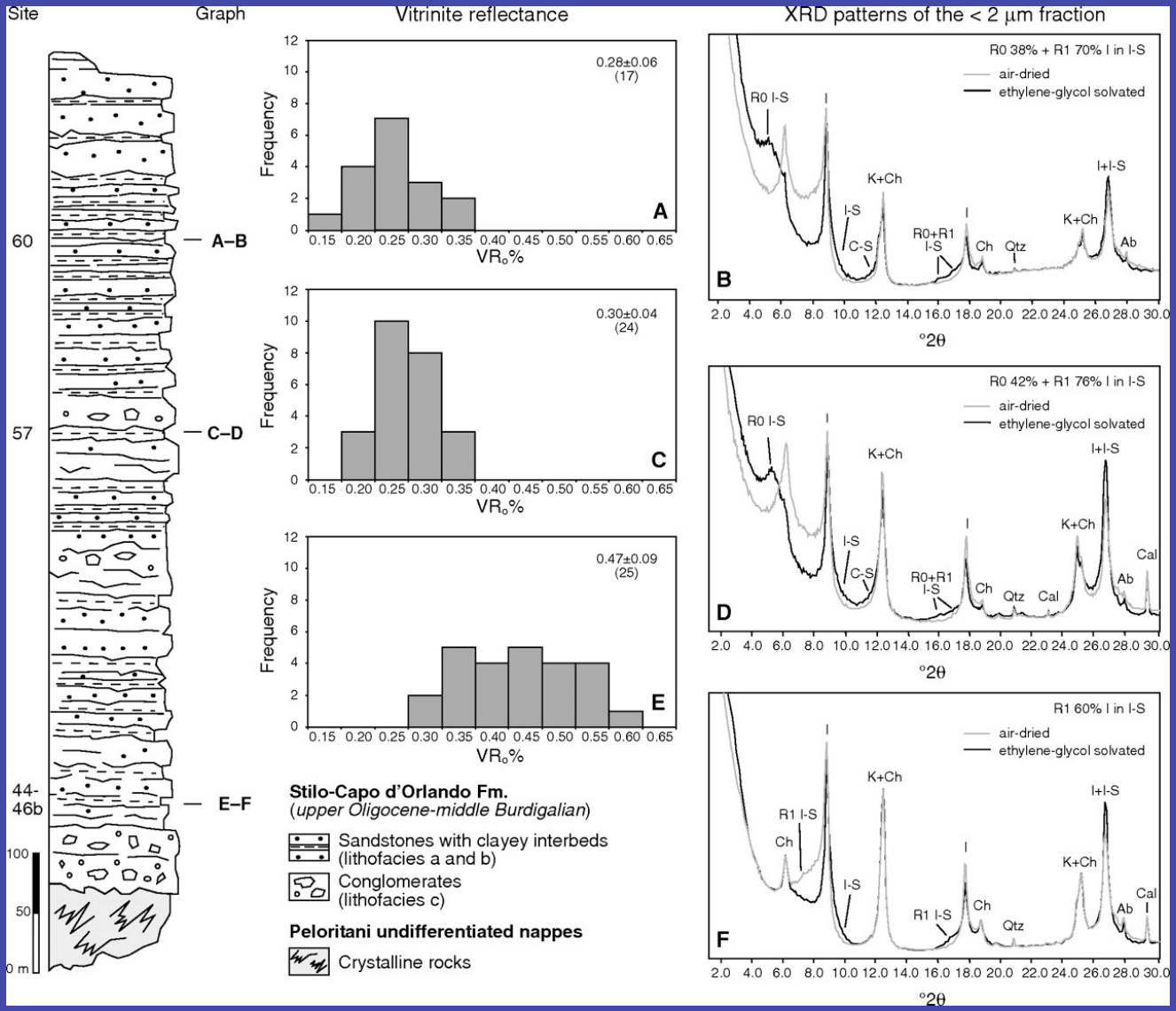

Aldega L et al. Geological Society of America Bulletin 2010;123:132-149

Sketch maps of the Peloritani Mountains with distribution of vitrinite reflectance (A), illite content in mixed-layer I-S (B), and apatite fission-track data (C) from Thomson (1994; italics) and Balestrieri et al.

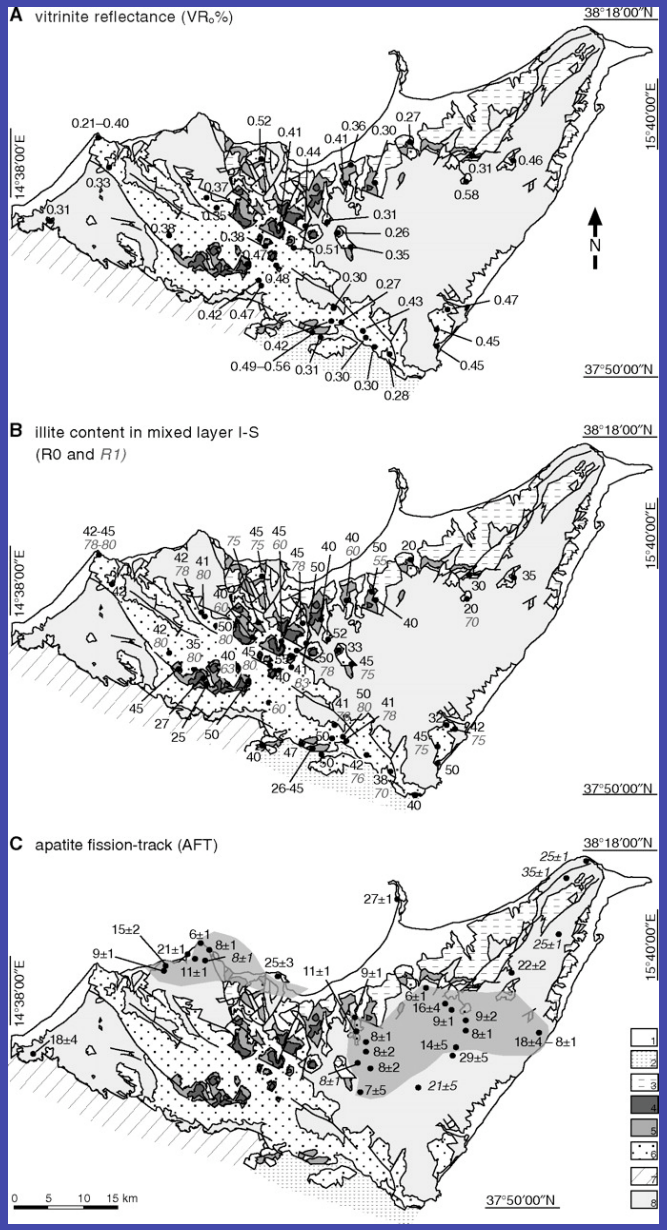

Aldega L et al. Geological Society of America Bulletin 2010;123:132-149

Synthetic stratigraphic logs of the Serravallian-Messinian deposits and the Antisicilide unit + Calcareniti di Floresta pair with selected vitrinite reflectance histograms (A–C) and X-ray diffraction (XRD) oriented patterns of the <2 µm grain-size fraction ...

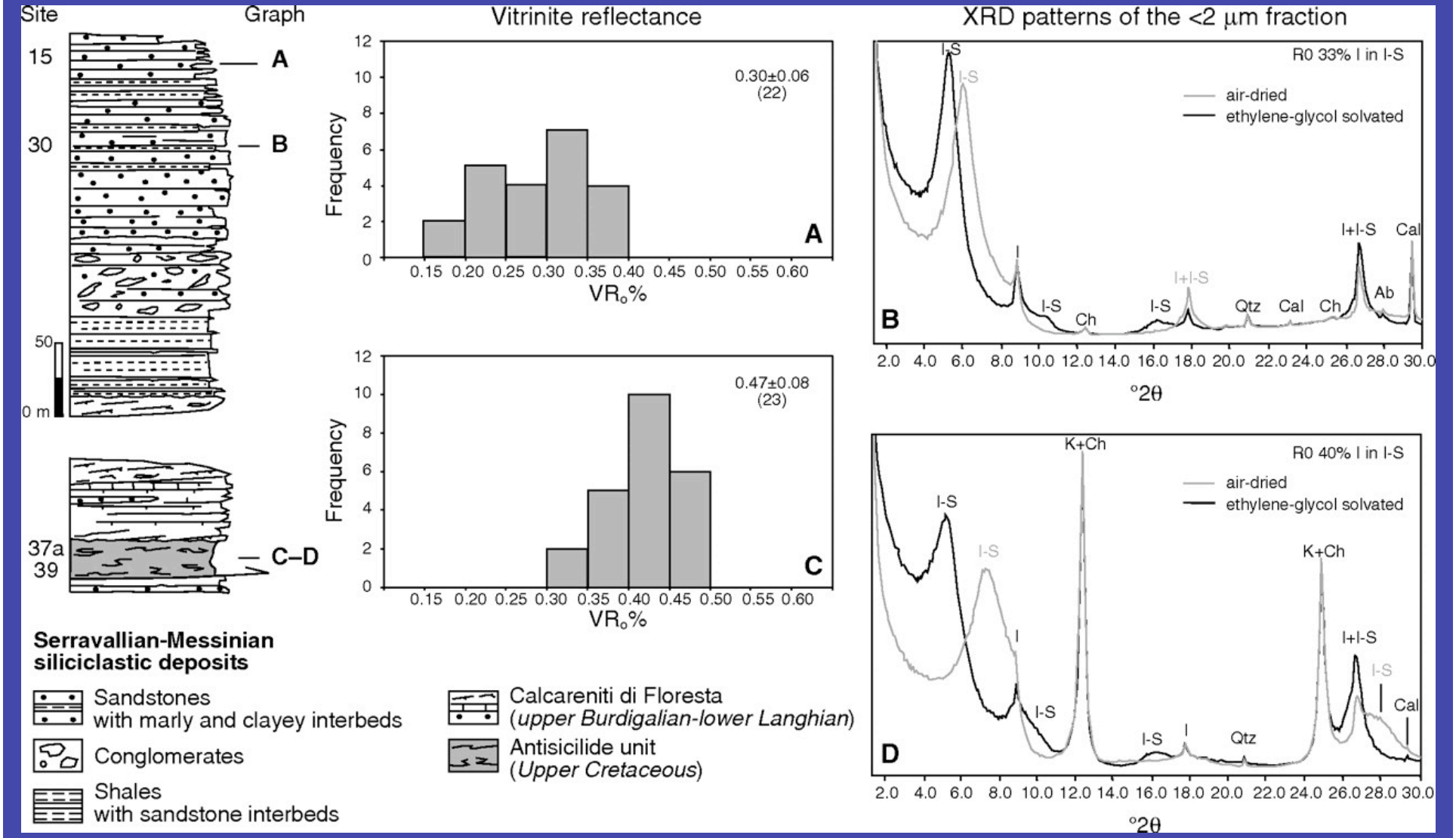

Aldega L et al. Geological Society of America Bulletin 2010;123:132-149

Low- and high-angle normal faults (A–D) and apparent reverse faults (E) in the Serravallian-Messinian deposits.

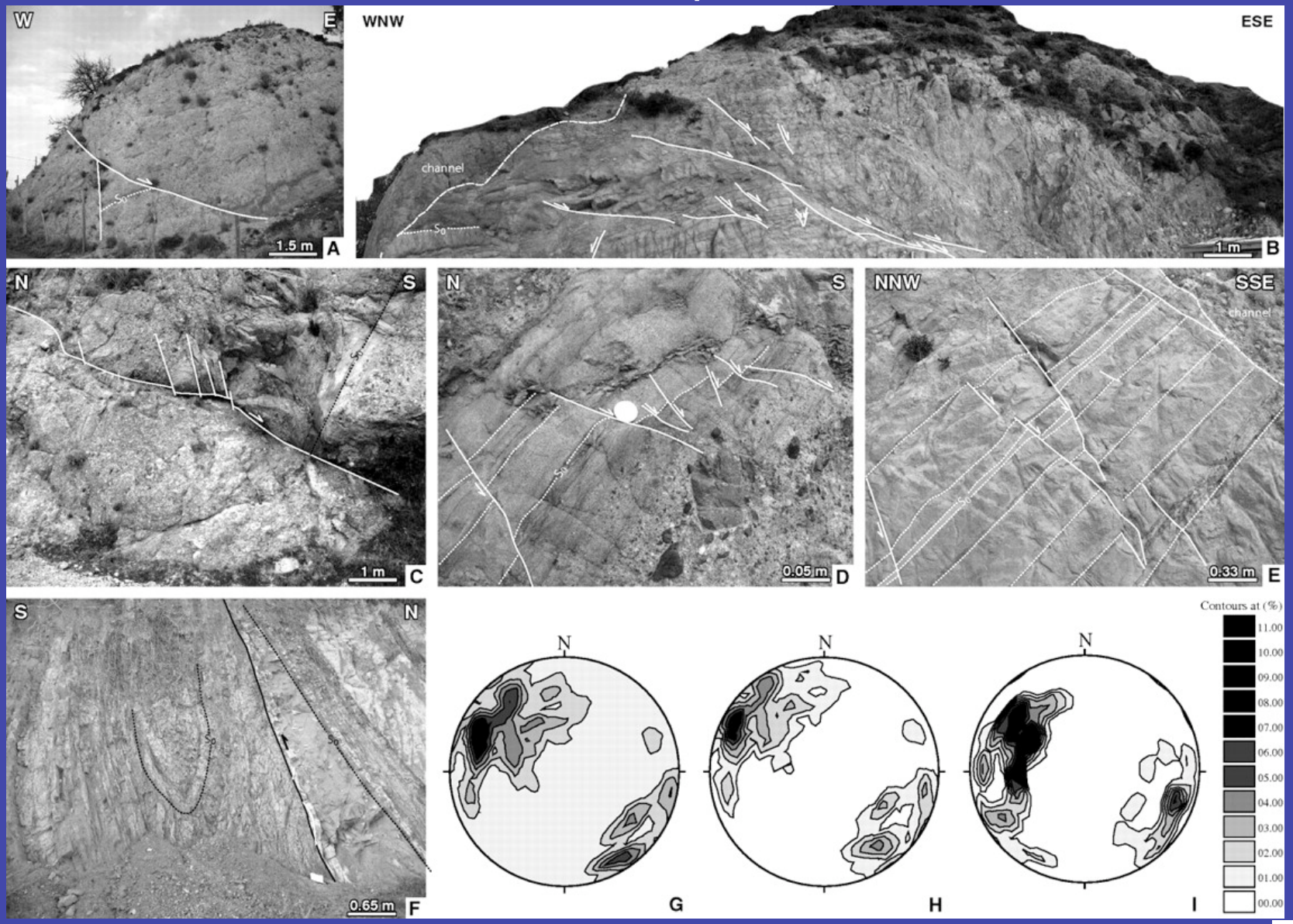

Aldega L et al. Geological Society of America Bulletin 2010;123:132-149

Isopach map of the paleodistribution of the Stilo-Capo d'Orlando Formation.

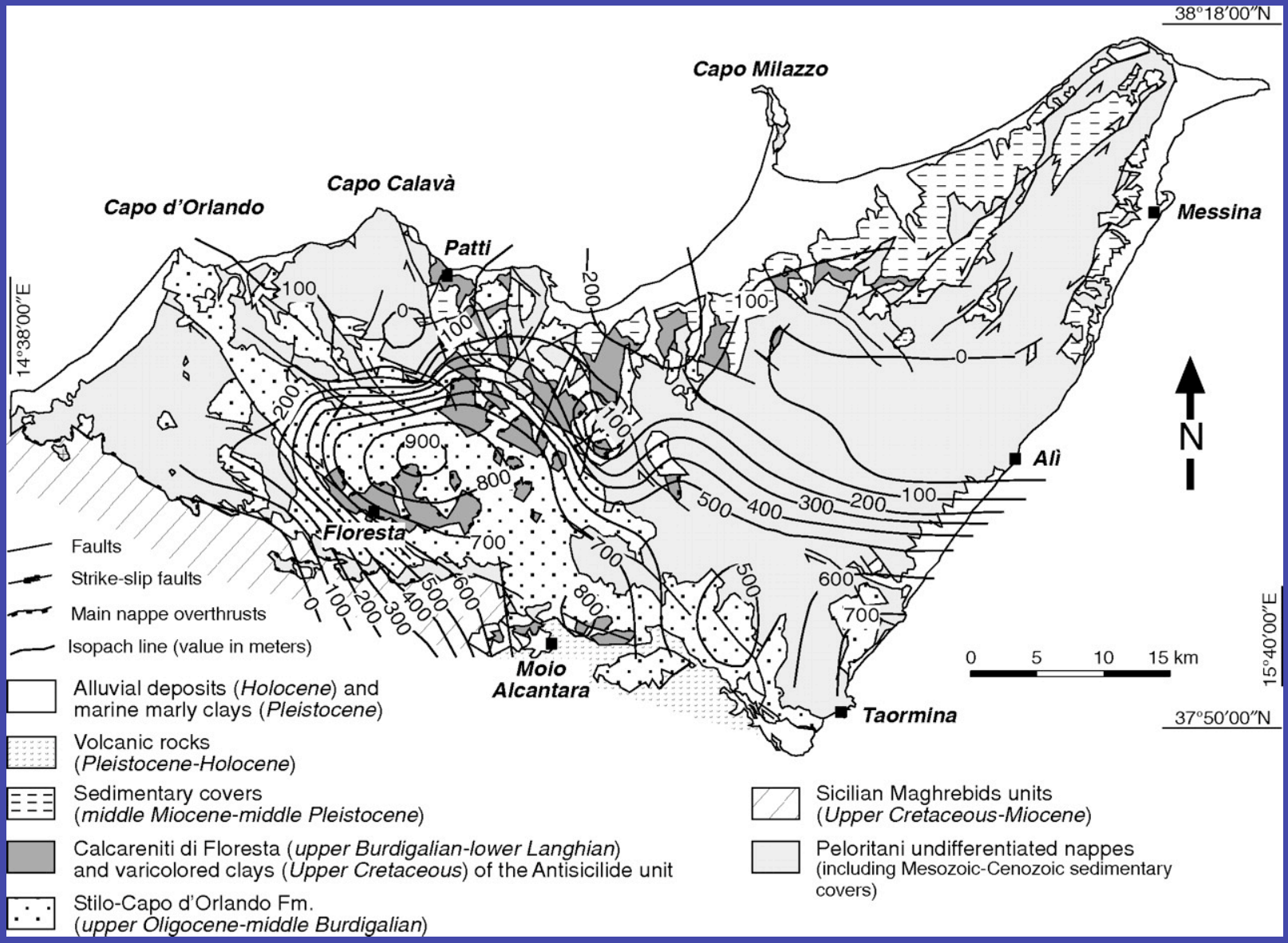

Aldega L et al. Geological Society of America Bulletin 2010;123:132-149

Heating rate values for the Stilo-Capo d'Orlando Formation extracted from the correlation of vitrinite reflectance and expandability (reverse of illite content in illite-smectite [I-S]) data based on the kinetic model of vitrinite maturation of Burnham and ...

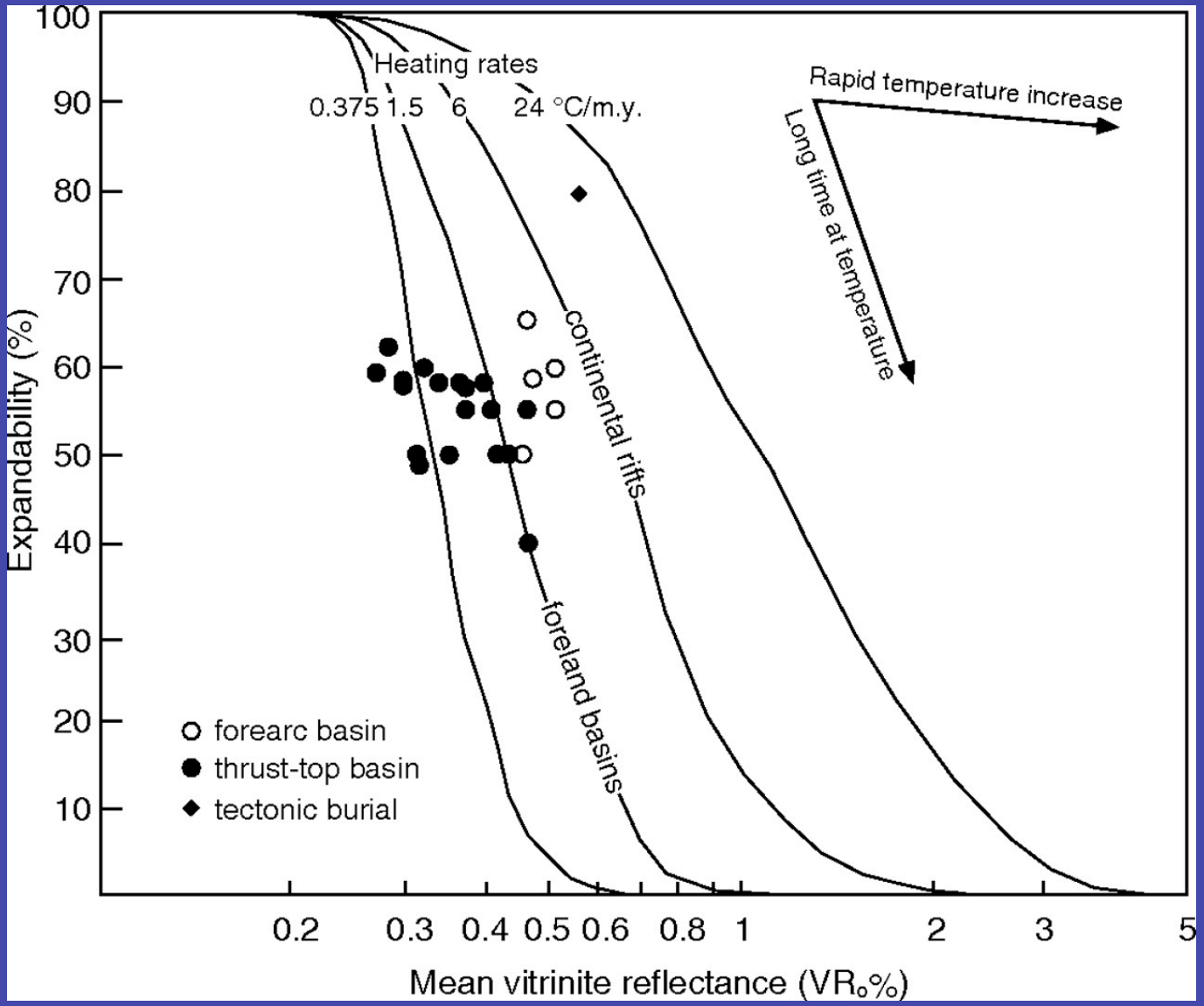

Aldega L et al. Geological Society of America Bulletin 2010;123:132-149

(A) Representative one-dimensional (1-D) burial and thermal modeling of the Stilo-Capo d'Orlando Formation in the basin depocenter.

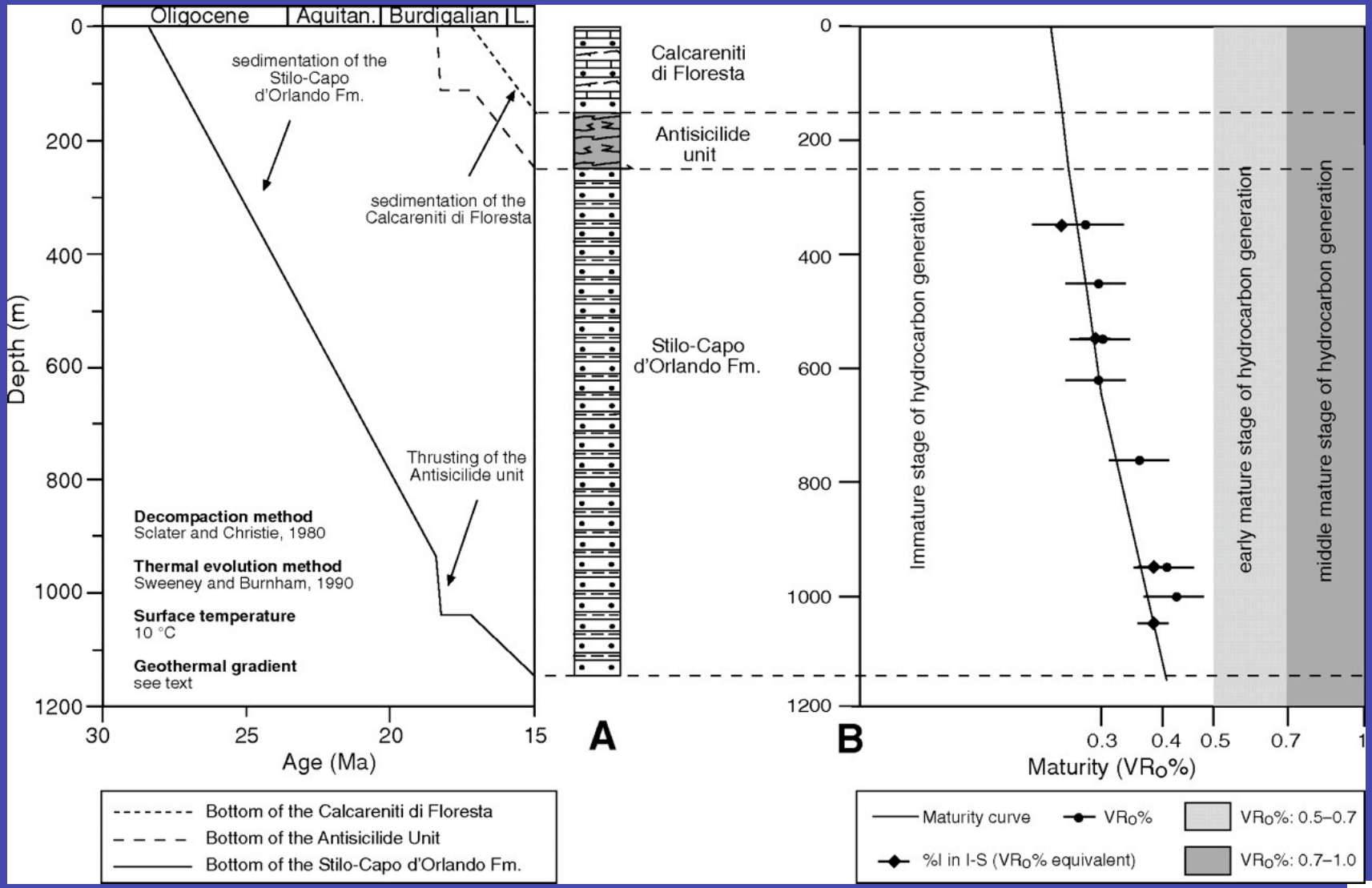

Aldega L et al. Geological Society of America Bulletin 2010;123:132-149

Schematic evolution of burial-exhumation of the Peloritani Mountains since the middle Miocene: (A) early Langhian; (B) late Langhian–(?)early Serravallian; and (C) early Messinian–Quaternary.

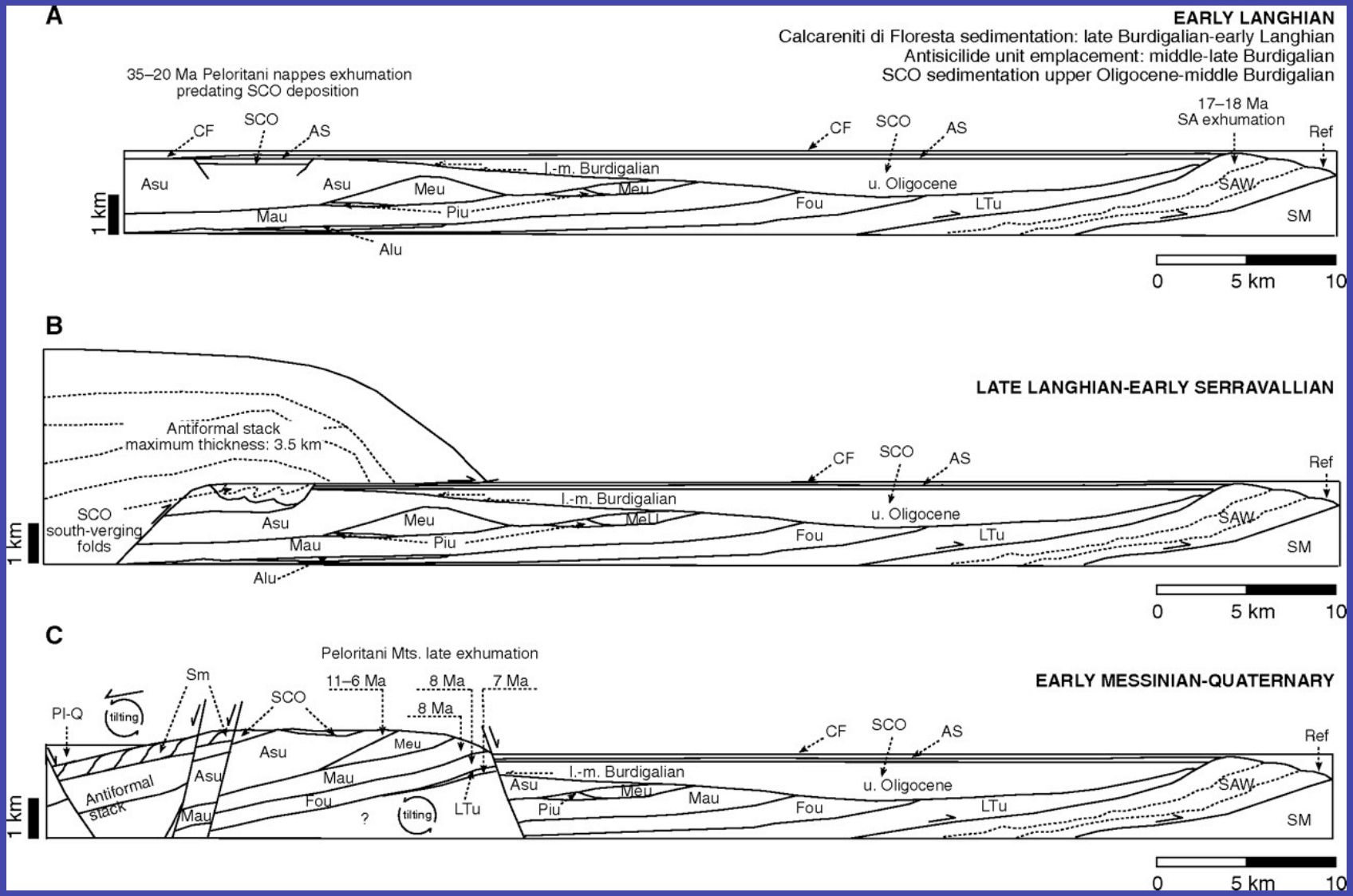

Aldega L et al. Geological Society of America Bulletin
2010;123:132-149

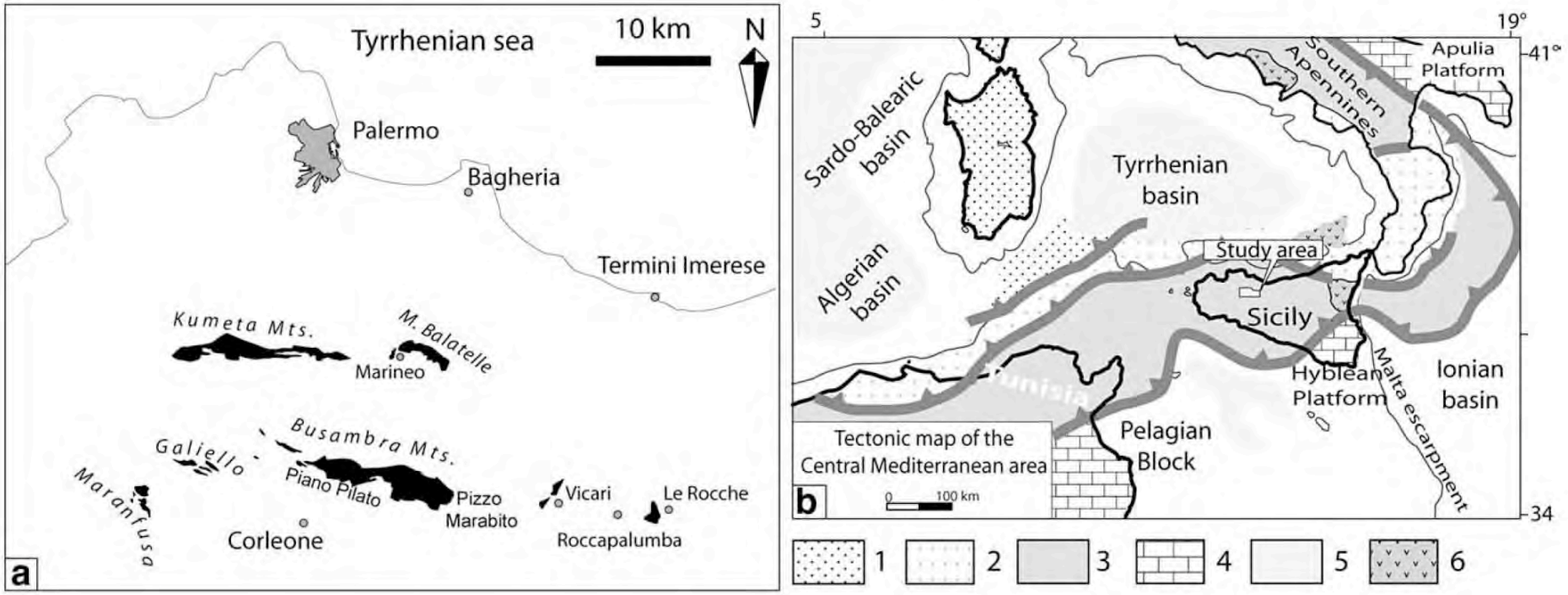

Fig. 1. a) Distribution of the Jurassic–Cretaceous Trapanese pelagic carbonate platform rock successions in central-western Sicily. b) Tectonic map of the central Mediterranean (modified from Catalano et al., 2000), 1 Corsica–Sardinia domain; 2 Calabro–Kabilian Arc, "internal" Flysch sequences, ophiolites; 3 Maghrebian–Sicilian–South Apennine Chain and deformed foreland; 4 undeformed foreland (Tunisia, Hyblaean Plateau, Apulia); 5 Extensional areas ; 6 Plio-Quaternary volcanics.

Basilone et al 2010

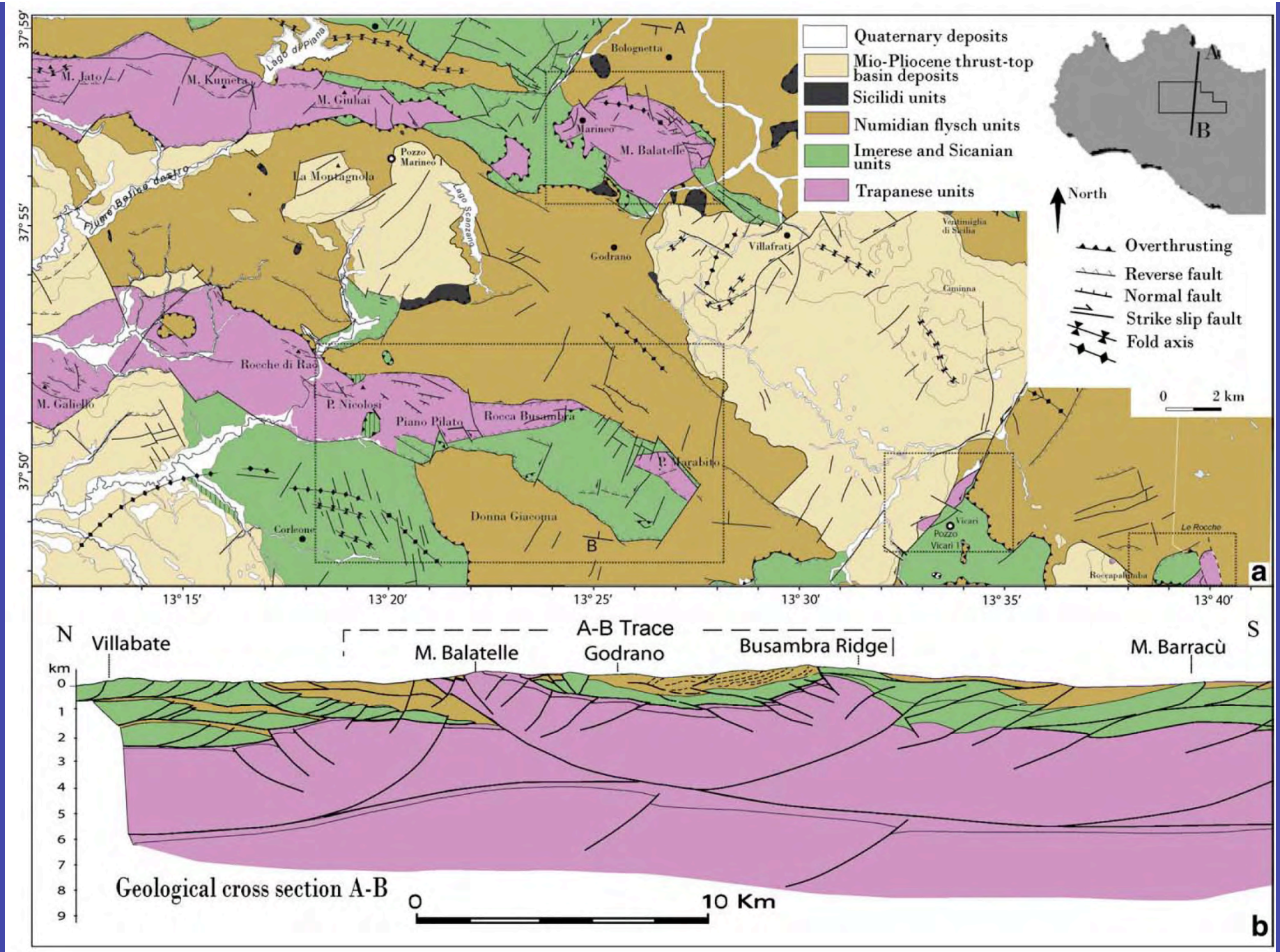

Basilone et al 2010

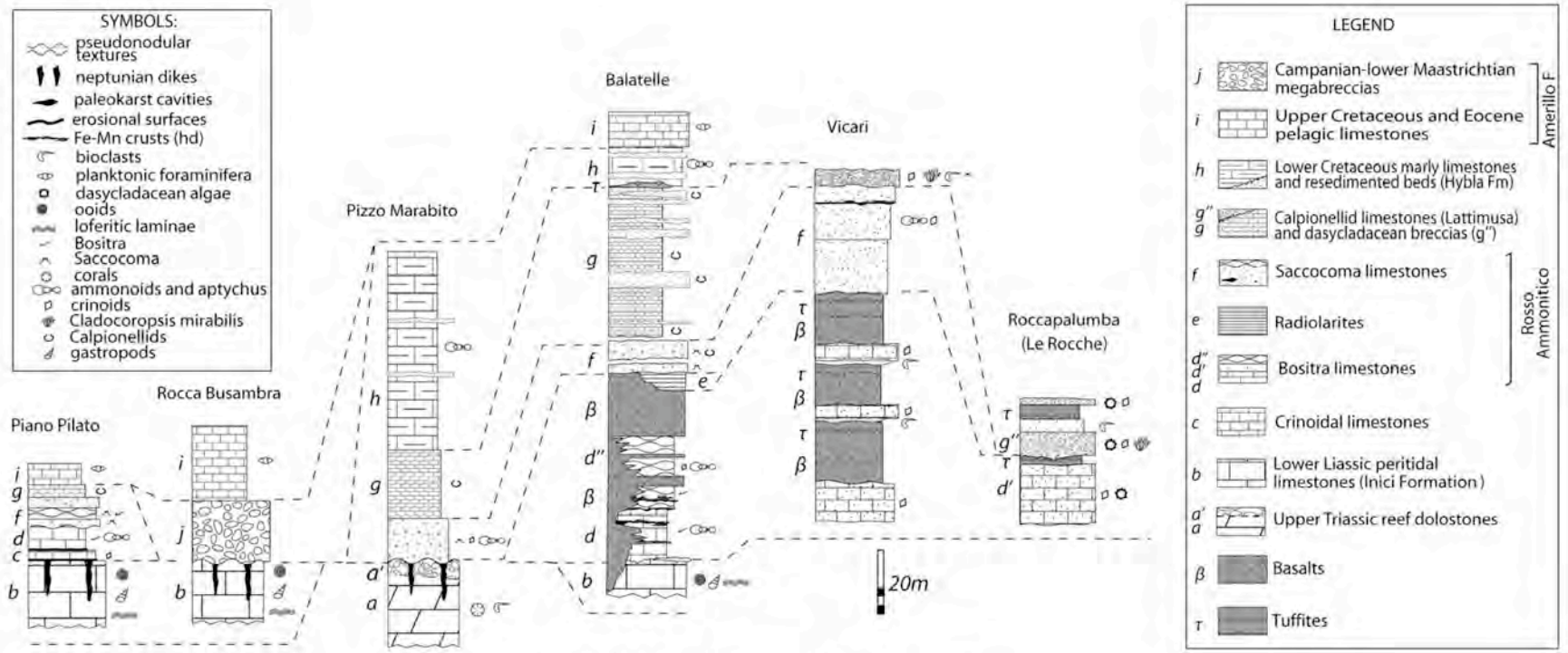

Fig. 3. Stratigraphic columns of the study successions.

Basilone et al 2010

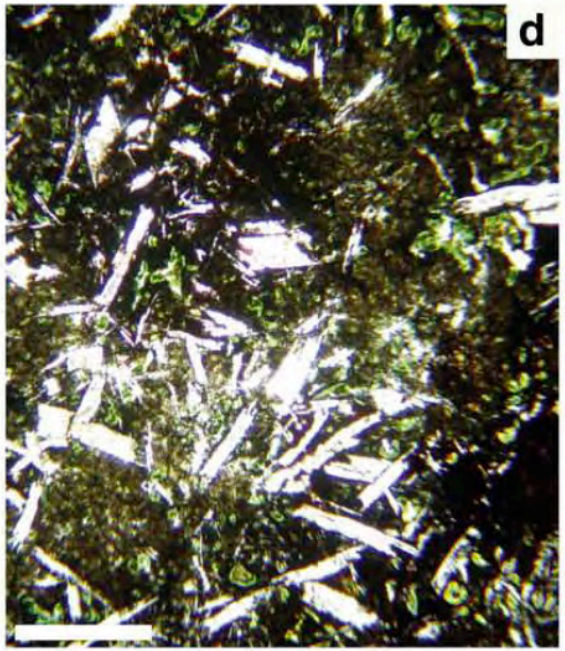

Basilone et al 2010

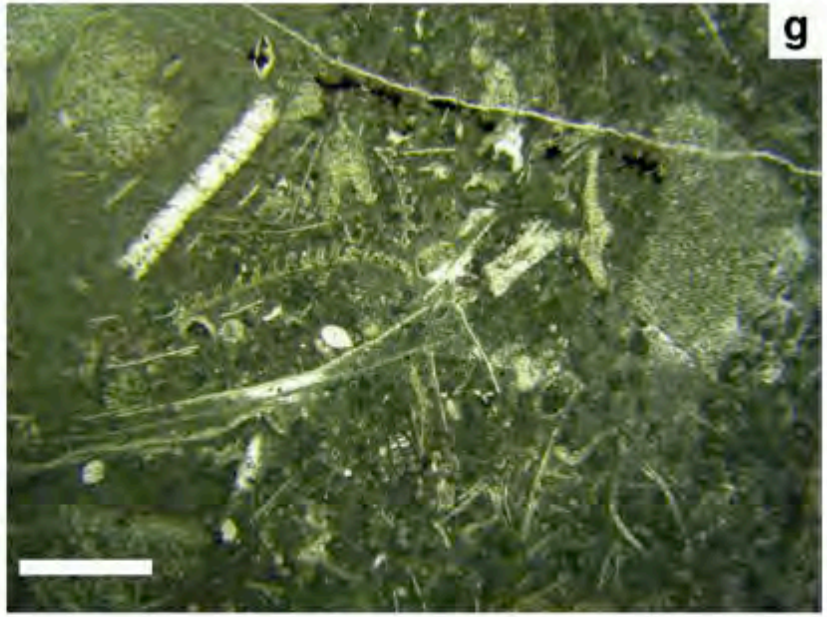

Fig. 4. Characteristic facies and microfacies of the Jurassic study successions: a) Fe–Mn nodules and dark crusts of the *Bositra* limestones (lower Rosso Ammonitico mb of the Buccheri Fm, Rocca Busambra); b) bioclastic wackestone, with benthic foraminifera, pelagic bivalves and thick-shelled mollusca fragments, often Mn-coated (*Bositra* limestones, Rocca Busambra, PPL, scale bar 1 mm); c) thick body of basaltic pillow lava interlayered in the *Bositra* limestones of Monte Balatelle; d) darkish basalts interlayered in the Jurassic succession of Monte Balatelle (sample from well, PPL, scale bar 1 mm); e) crossed laminated tuffitic sands enclosed between basalts (below) and the Bajocian–Bathonian limestones of the Vicari succession (above); f) Middle Jurassic red basaltic pillow lavas (Monte Balatelle); g) wackestone–packstone with benthic foraminifera, *Aptychus*, bryozoans, calpionellids, thin- and thick-shelled bivalve fragments, crinoids (*Saccocoma* limestones, Pizzo Marabito, Rocca Busambra, PPL, scale bar 1 mm).

Basilone et al 2010

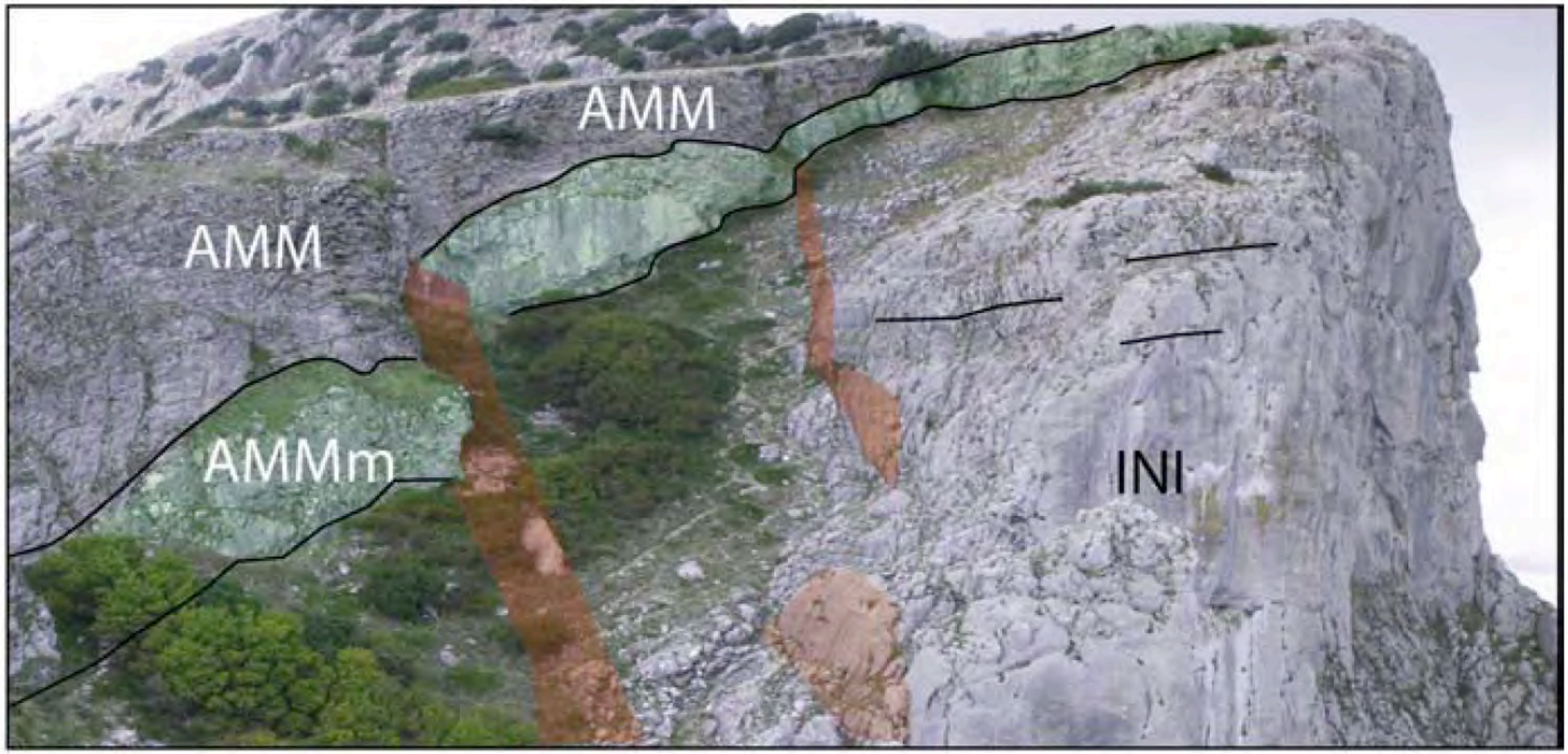

Fig. 6. Faulted massive Upper Cretaceous megabreccias (AMMm, in light green) and upward thin Upper Cretaceous–Eocene pelagic beds (AMM) that onlap and abut, in buttress unconformity, the faulted Lower Jurassic peritidal limestones (INI; fault planes are in red, modif. From Basilone 2009).

Basilone et al 2010

Fig. 7. a) Large fracture set on the Inici Fm limestones (INI) filled by basaltic pillow lavas (β; Monte Balatelle). This fracture set cuts an inherited normal fault and is covered, in buttress unconformity, by the Middle Jurassic *Bositra* limestones (d); b) details of the buttress unconformity.

Basilone et al 2010

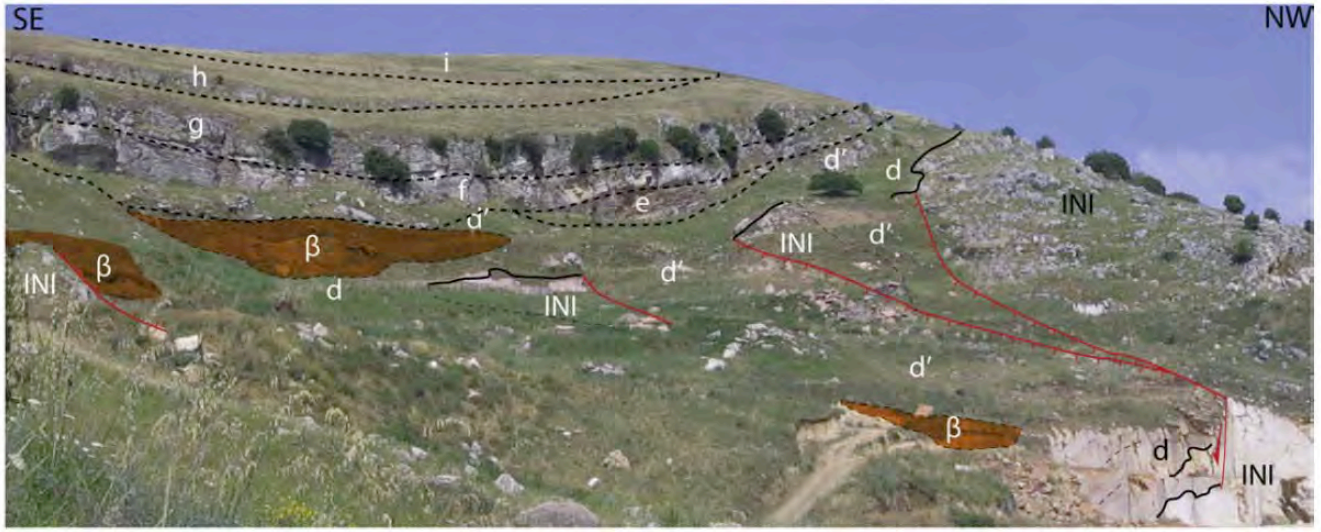

Fig. 8. Panoramic view of the eastern side of Monte Balatelle showing E–Woriented normal faults (red lines), cutting the Lower Jurassic Inici Fm limestones (INI). The conjugate dip–slip fault system, produced an E–W oriented graben structure filled by Middle Jurassic lower Rosso ammonitico mb of the Buccheri Fm, consisting of Bositra limestones (d) and nodular limestones (d′), that onlap in buttress unconformity and rest above the faulted Inici Fm beds. Pillow lava intercalations (β) are also present. The tectonic depression is sealed by the radiolaritic member (e) and by the Saccocoma limestones (f). The calpionellid limestones (g, Lattimusa), the Hybla (h) and the Amerillo (i) Fms seal the above-mentioned

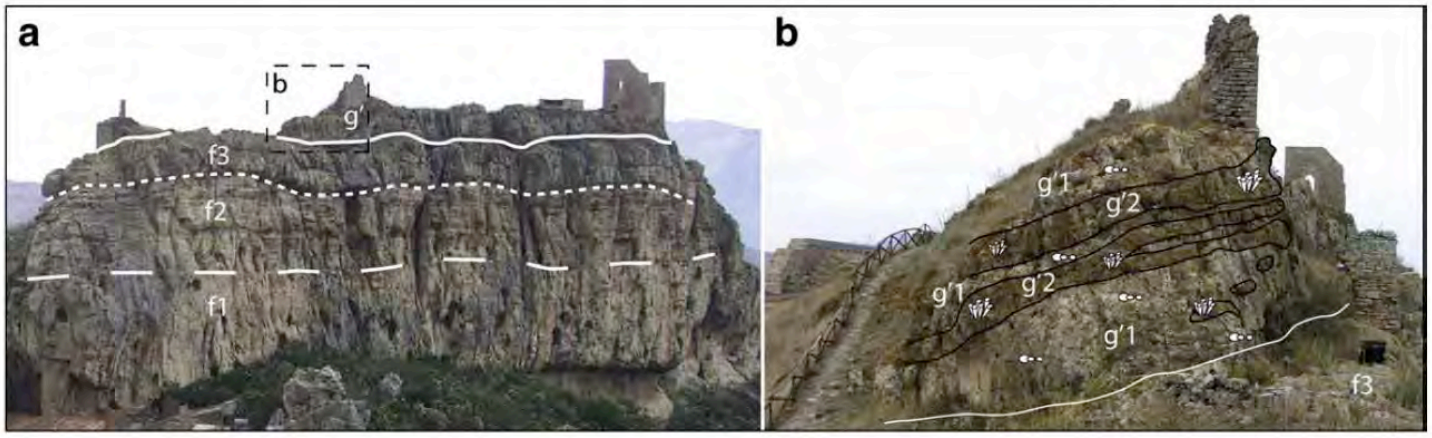

Fig. 9. Upper Jurassic succession outcropping at Vicari Castle. a) The "*Cladocoropsis* breccias" (g′) cover, unconformably the eroded uppermost member of the Buccheri Fm: *Saccocoma* limetsones (f1); wackestone with reworked ammonites and reef-derived elements (f2); fine conglomerates with erosional lower boundary (f3). b) Detail of the same site, which shows the relations of the different lithofacies forming the "*Cladocoropsis* breccias" unit: packstone with reworked ammonites (g′1); rudstone with large carbonate reef-derived elements (g′2).

Basilone et al 2010

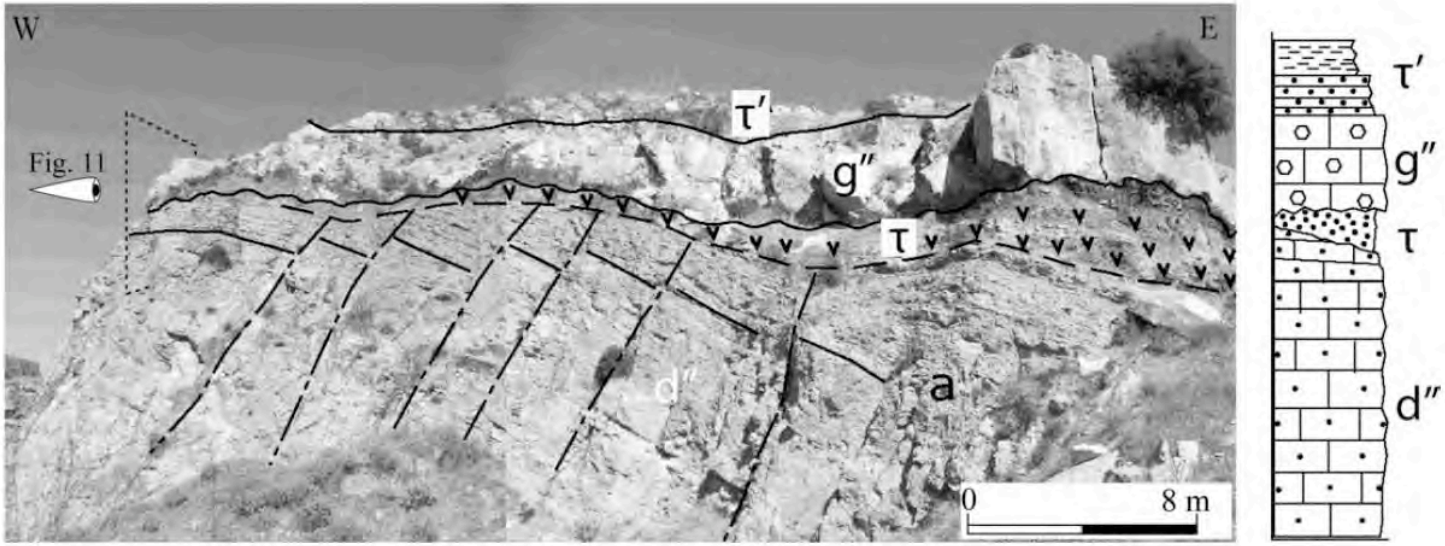

Fig. 10. Le Rocche di Roccapalumba quarry. Faulted and tilted Middle Jurassic crinoidal grainstone (d″) pertains to the lower mb of the Buccheri Fm. Bajocian volcanite intercalations (τ) are capped, with erosion, by the massive Lower Cretaceous "*Dasycladacean* breccias" (g″) and by grey packstone and fine tuffites (τ).

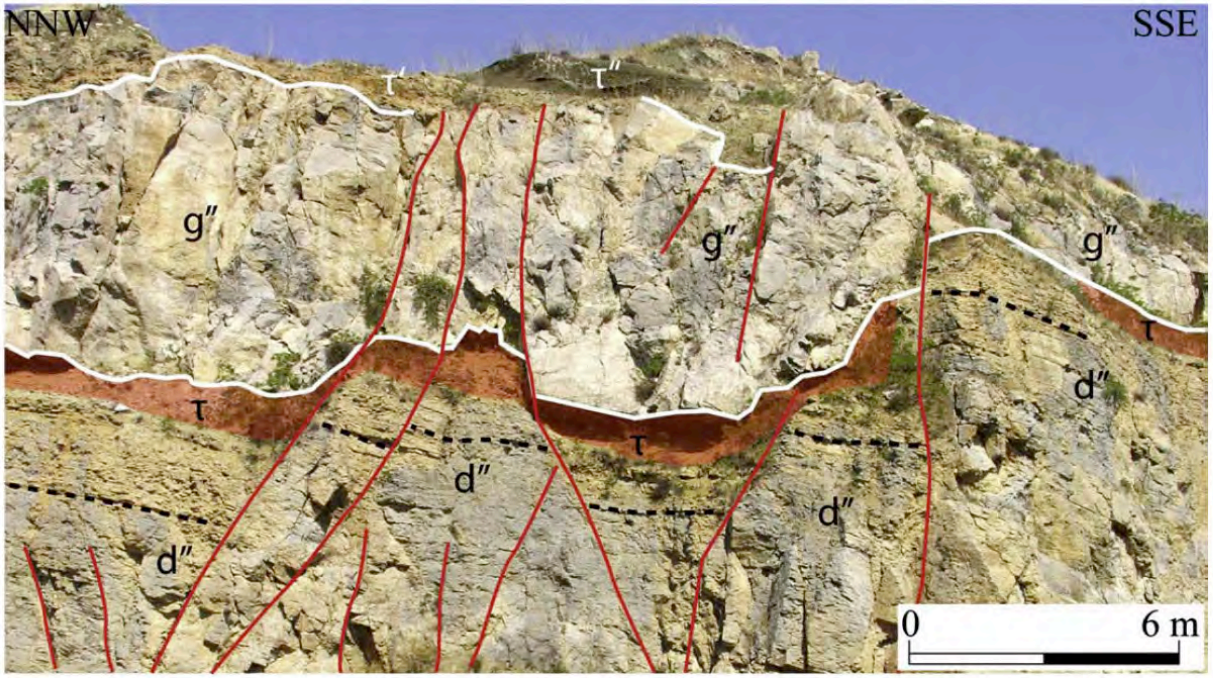

Fig. 11. Details of the previous figure, showing the buttress unconformity between the faulted deposits (crinoidal grainstone, d″) and the overlaying Lower Cretaceous "*Dasycladacean* breccias" (g″). Interlayered red volcaniclastic material (τ) is also evident.

Basilone
et al 2010

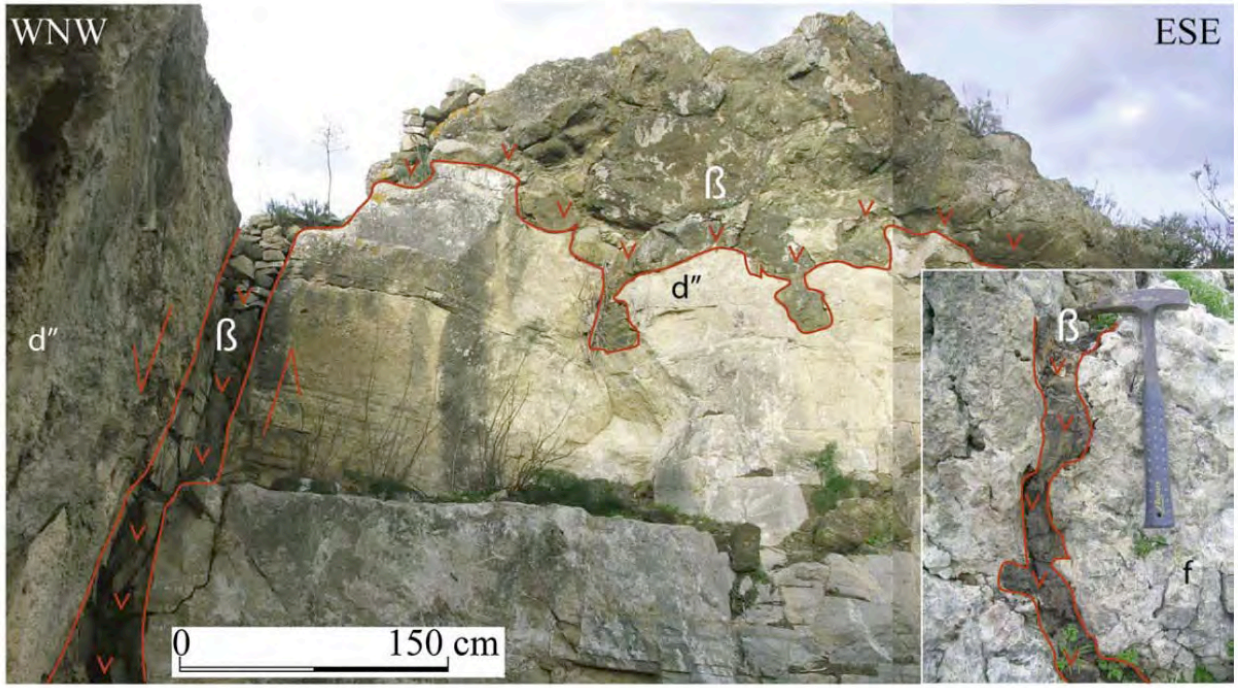

Fig. 13. Pizzo Falconiere, Vicari. NNE–SSW normal fault filled by basalts (β), that in turn, unconformably cover the Middle Jurassic laminated crinoidal grainstone (d″).

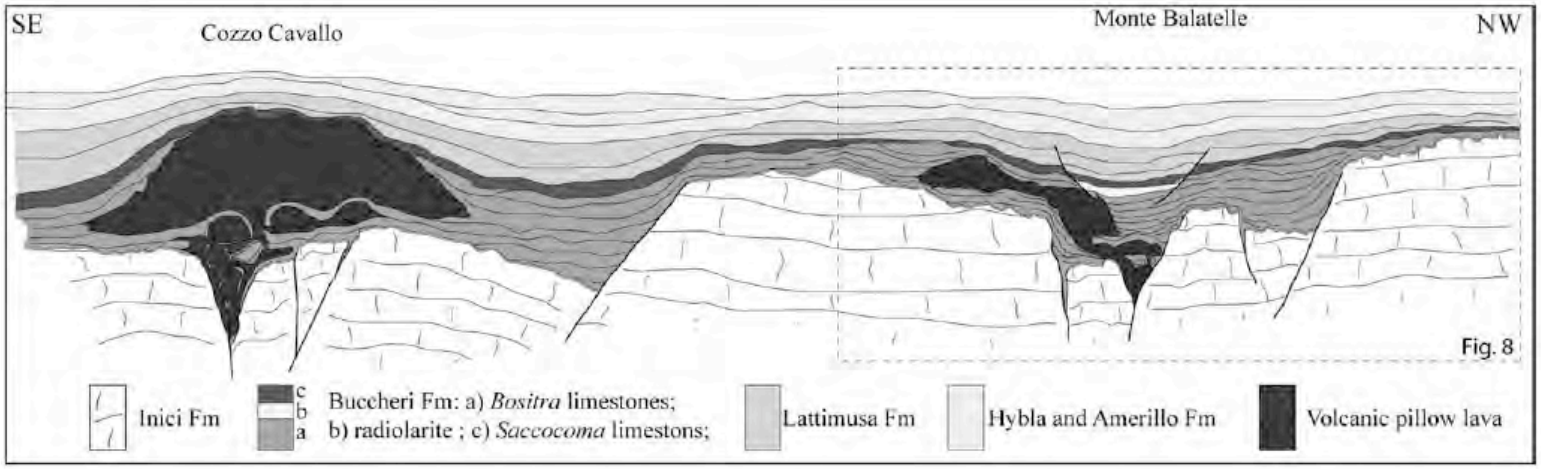

Fig. 15. Schematic cross-section along the Monte Balatelle–Cozzo Cavallo E–W alignment, showing the tectonic–stratigraphic relationships between the Jurassic Buccheri Fm deposits and the interlayered igneous rocks. Lower Jurassic faults have been the origin of the main graben structures, filled by the Jurassic–Lower Cretaceous pelagic deposits of the Buccheri, Lattimusa and Hybla Fms.

Basilone
et al 2010

Basilone
et al 2010

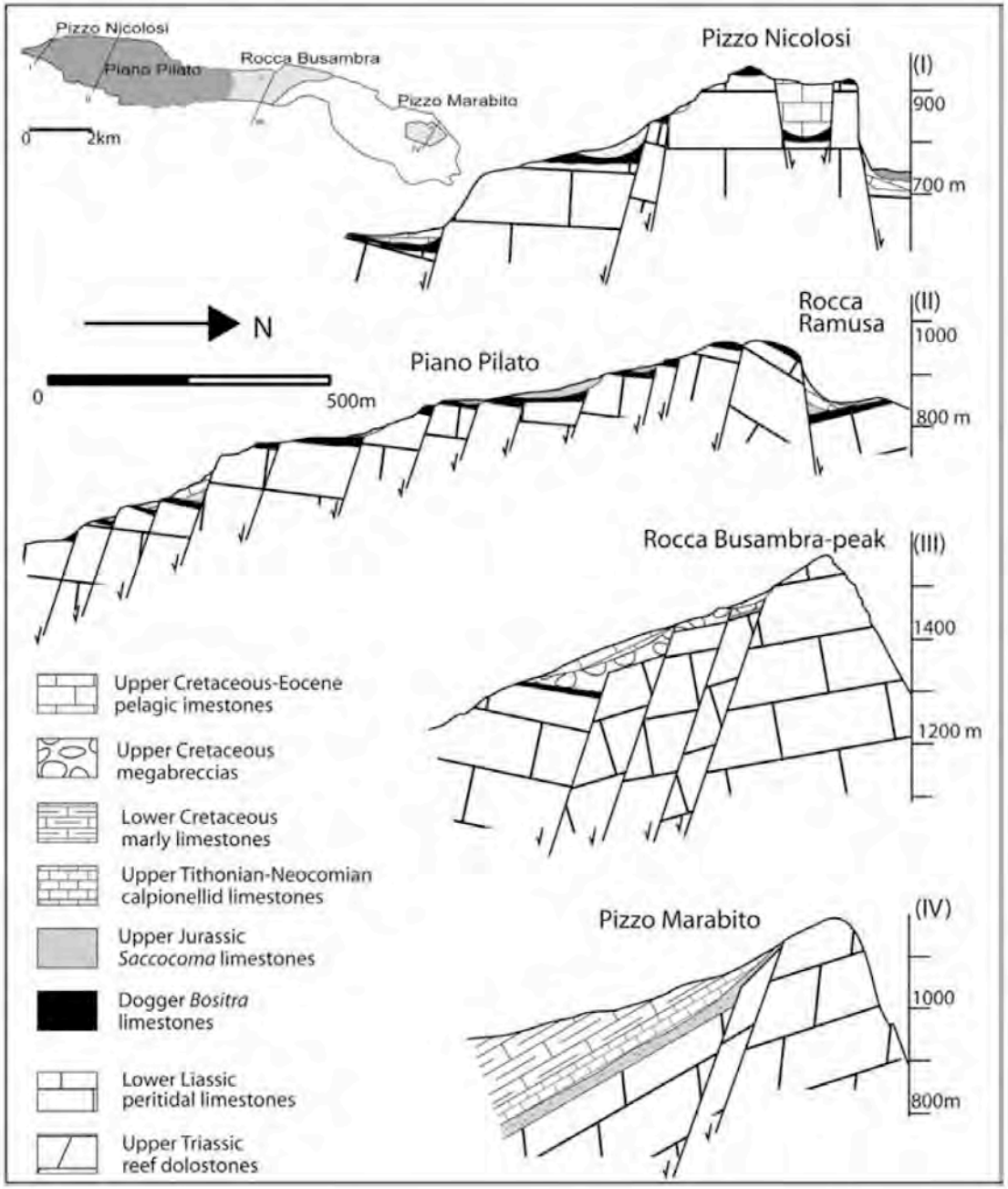

Fig. 14. NNE–SSW tectonic profiles, showing the depositional setting of different areas of the Rocca Busambra ridge (modified from Basilone, 2009).

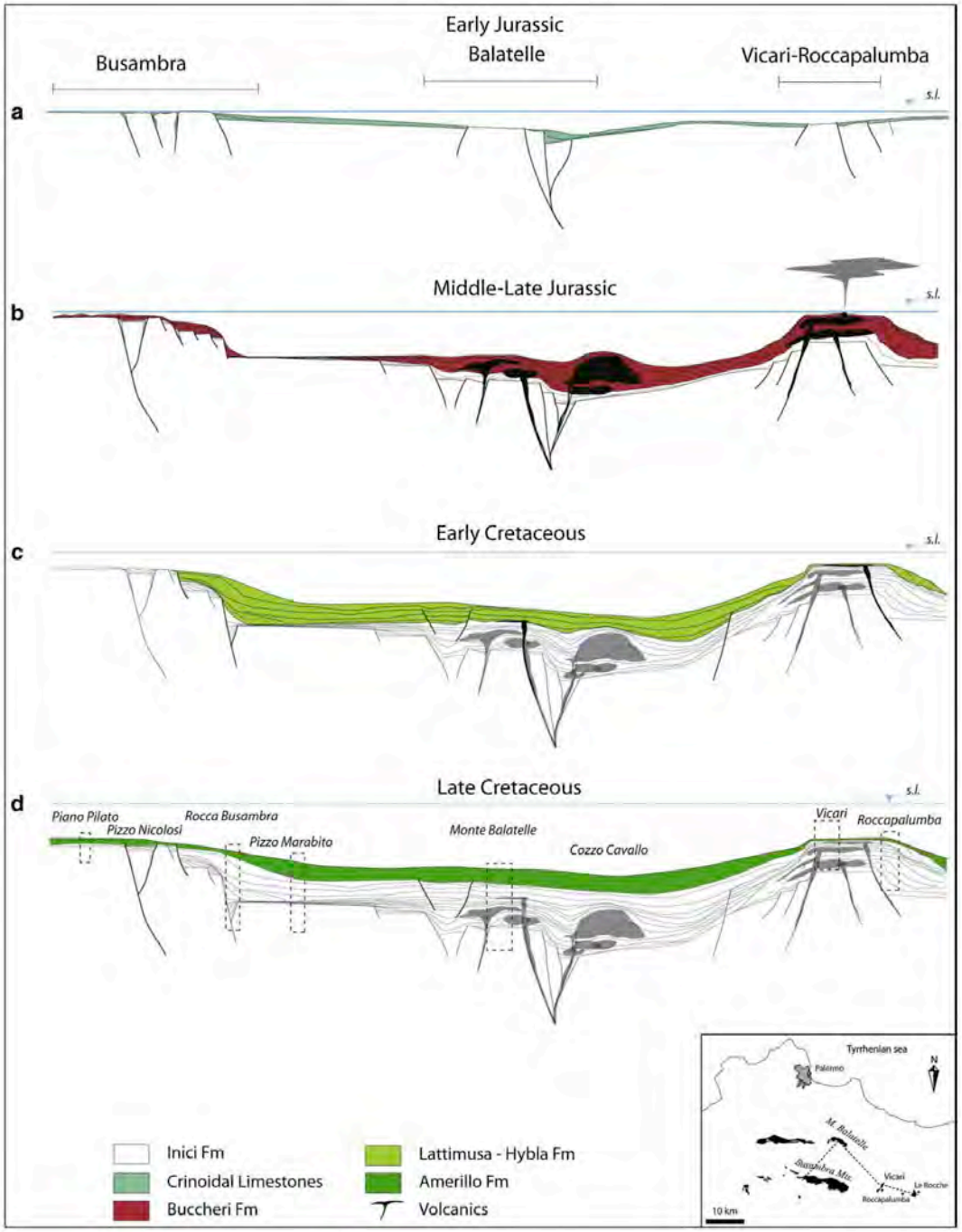

Fig. 16. Essay of paleogeographic restoration of the study sectors of the Trapanese domain during the Mesozoic.

Basilone
et al 2010

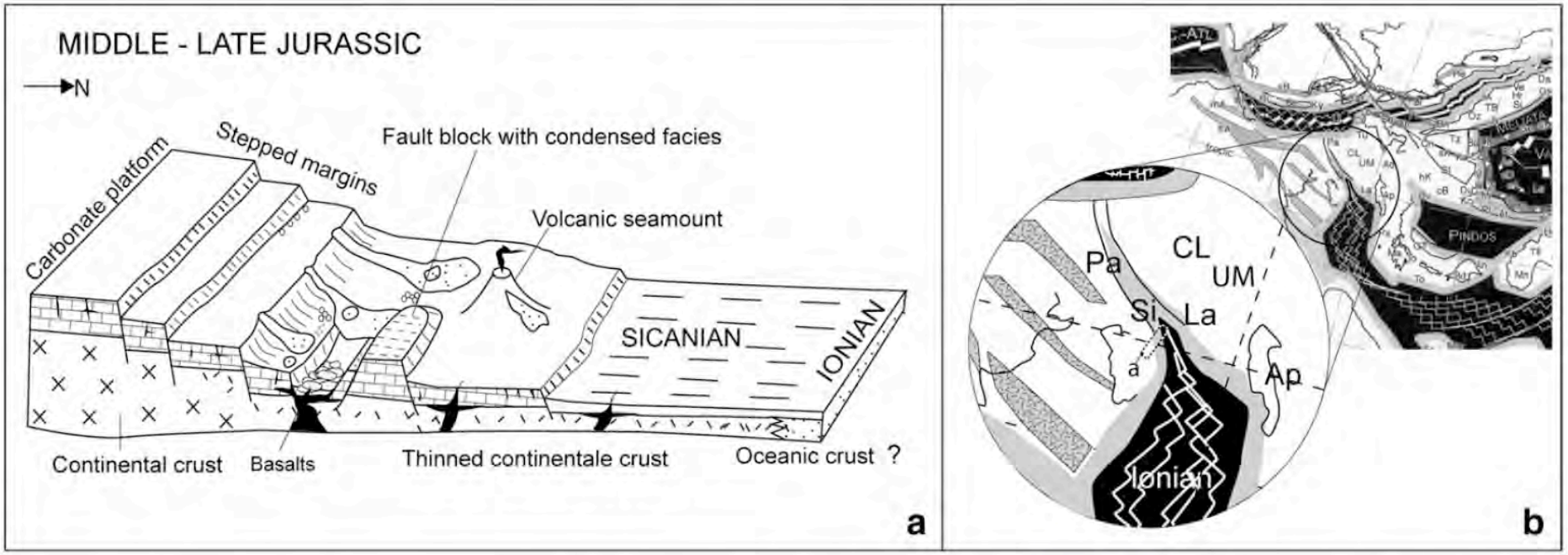

Fig. 17. a) Interpretative diagram showing the tectono-sedimentary setting of the study areas and the main factors influencing the deposition, during the Middle–Late Jurassic; b) Palaeogeography of the European–Mediterranean area during the Middle–Late Jurassic (modified after Stampfli and Borel, 2002) with location of the study sectors.

Basilone
et al 2010